

Introduction to Cluster Algebras

Chapter 7

(preliminary version)

SERGEY FOMIN

LAUREN WILLIAMS

ANDREI ZELEVINSKY

Preface

This is a preliminary draft of Chapter 7 of our forthcoming textbook *Introduction to cluster algebras*, joint with Andrei Zelevinsky (1953–2013).

Other chapters have been posted as

- (Chapters 1–3),
- (Chapters 4–5), and
- (Chapter 6).

We expect to post additional chapters in the not so distant future.

Anne Larsen and Raluca Vlad made a number of valuable suggestions that helped improve the quality of the first version of this manuscript. We are also grateful to Zenan Fu, Amal Mattoo, Hanna Mularczyk, and Ashley Wang for their comments on a subsequent version of this chapter, and for assistance with creating figures, and to Gregory Li, Stella Li, Annabel Ma, Jacob Paltrowitz, and Katherine Tung for their comments on the current version of this chapter and assistance with figures. We would also like to thank Melissa Sherman-Bennett for useful comments. Last but not least, we are grateful to Pasha Galashin, whose suggestions greatly clarified our exposition.

Our work was partially supported by the NSF grants DMS-1664722, DMS-1854512, DMS-1854316, DMS-2054231, DMS-2152991, DMS-2348501, and by the Radcliffe Institute for Advanced Study.

Comments and suggestions are welcome.

Sergey Fomin
Lauren Williams

2020 *Mathematics Subject Classification*. Primary 13F60.

© 2021 by Sergey Fomin, Lauren Williams, and Andrei Zelevinsky

Contents

Chapter 7. Plabic graphs	1
§7.1. Plabic graphs and the main results	3
§7.2. Plabic graphs and their quivers	9
§7.3. Triangulations and wiring diagrams via plabic graphs	11
§7.4. Trivalent plabic graphs	15
§7.5. Triple diagrams and normal plabic graphs	19
§7.6. Minimal triple diagrams	28
§7.7. From minimal triple diagrams to reduced plabic graphs	36
§7.8. The bad features criterion	39
§7.9. Affine permutations	41
§7.10. Bridge decompositions	46
§7.11. Edge labels of reduced plabic graphs	49
§7.12. Face labels of reduced plabic graphs	53
§7.13. Grassmann necklaces and weakly separated collections	57
Bibliography	61

Plabic graphs

In this chapter, we present the combinatorial machinery of *plabic graphs*, which were introduced by A. Postnikov [22]. These are planar (unoriented) graphs with bicolored vertices satisfying some mild technical conditions. Plabic graphs can be transformed using certain *local moves*. A key observation is that each plabic graph gives rise to a quiver, so that local moves on plabic graphs translate into (a subclass of) quiver mutations.

Crucially, the combinatorics underlying several important classes of cluster structures that arise in applications fits into the plabic graphs framework. This in particular applies to the basic examples introduced in Chapter 1. More concretely, we show that the combinatorics of flips in triangulations of a convex polygon (resp., braid moves in wiring diagrams, either ordinary or double) can be entirely recast in the language of plabic graphs. In these and other examples, an important role is played by the subclass of *reduced* plabic graphs that are analogous to—and indeed generalize—reduced decompositions in symmetric groups.

D. Thurston’s *triple diagrams* [25] are closely related to plabic graphs. After making this connection precise and developing the machinery of triple diagrams, we use this machinery to establish the fundamental properties of reduced plabic graphs.

Plabic graphs and related combinatorics have arisen in the study of shallow water waves [17, 18] (via the KP equation) and in connection with scattering amplitudes in $\mathcal{N} = 4$ super Yang-Mills theory [2]. Constructions closely related to plabic graphs were studied by T. Kawamura [14] in the context of the topological theory of graph divides.

A reader interested exclusively in the combinatorics of plabic graphs can read this chapter independently of the previous ones. While we occasionally

refer to combinatorial constructions introduced in Chapters 1–2, they are not relied upon in the development of the general theory of plabic graphs.

Cluster algebras as such do not appear in this chapter. On the other hand, as we will see in a subsequent chapter, reduced plabic graphs introduced herein will prominently feature in the study of cluster structures in Grassmannians and related varieties. A reader who wishes to skim the chapter for the main ideas may choose to read only Sections 7.1– 7.3, and Sections 7.11–7.13.

The structure of this chapter is as follows.

In Section 7.1 we introduce plabic graphs and give an overview of the main results about them. In particular, we introduce the important notions of *reduced plabic graph* and *trip permutation*, and we state (but do not prove) the “fundamental theorem of reduced plabic graphs,” which characterizes the move-equivalence classes of reduced plabic graphs in terms of associated *decorated permutations*.

Section 7.2 describes how to associate a quiver to any plabic graph.

In Section 7.3, we recast the combinatorics of triangulations of a polygon and (ordinary or double) wiring diagrams in the language of plabic graphs.

Section 7.4 discusses the version of the theory in which all internal vertices of plabic graphs are *trivalent*. As Section 7.4 is not strictly necessary for the sections that follow, it can be skipped if desired.

Section 7.5 introduces the basic notions of *triple diagrams*. We then show that triple diagrams are in bijection with *normal plabic graphs*.

In Section 7.6, we study *minimal* triple diagrams, largely following [25]. These diagrams can be viewed as counterparts of reduced plabic graphs.

In Section 7.7, we explain how to go between minimal triple diagrams and reduced plabic graphs. We then use this correspondence to prove the fundamental theorem of reduced plabic graphs.

In Section 7.8, we state and prove the *bad features criterion* that detects whether a plabic graph is reduced or not.

In Section 7.9, we describe a bijection between decorated permutations and a certain subclass of *affine permutations*.

In Section 7.10, we use a factorization algorithm for affine permutations to construct a family of reduced plabic graphs called *bridge decompositions*.

Section 7.11 discusses *edge labelings* of reduced plabic graphs and gives the *resonance criterion* for recognizing whether a plabic graph is reduced.

Section 7.12 introduces *face labelings* of reduced plabic graphs.

In Section 7.13, we provide an intrinsic combinatorial characterization of collections of face labels that arise via this construction. Face labels will reappear in a subsequent chapter on cluster structures in Grassmannians.

7.1. Plabic graphs and the main results

Definition 7.1.1. A *plabic* (planar bicolored) *graph* is a (planar) graph G embedded into a closed disk \mathbf{D} , so that:

- the embedding of G into \mathbf{D} is planar, i.e., the edges do not cross;
- each internal vertex is colored black or white;
- each internal vertex is connected by a path to some boundary vertex;
- the (uncolored) vertices lying on the boundary of \mathbf{D} are labeled $1, 2, \dots, b$ in clockwise order, for some positive integer b ;
- each of these b *boundary vertices* is incident to a single edge.

Loops and multiple edges are allowed.

We consider plabic graphs up to isotopy of the ambient disk \mathbf{D} , fixing the disk's boundary. The *faces* of G are the connected components of the complement of G inside \mathbf{D} . A degree 1 internal vertex that is connected by an edge to a boundary vertex is called a *lollipop*. Any other degree 1 internal vertex is called a *leaf*. Boundary vertices are not leaves.

Two examples of plabic graphs are shown in Figure 7.1. Many more examples will appear throughout this chapter. In what follows, we will often omit the boundary of the ambient disk when drawing plabic graphs.

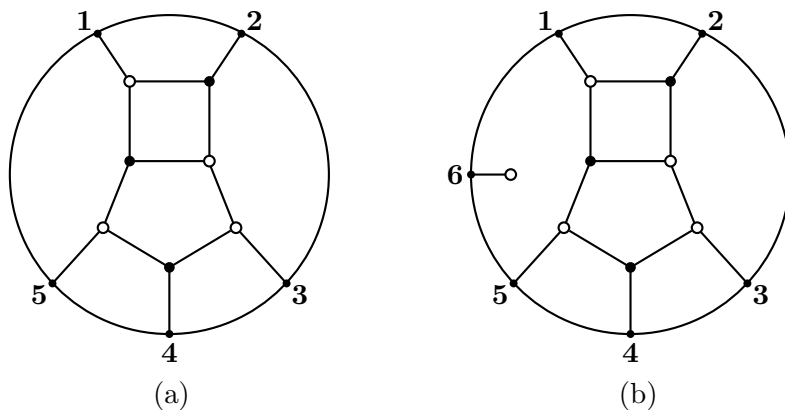


Figure 7.1. (a) A plabic graph G . (b) A plabic graph G' with a white lollipop.

Remark 7.1.2. Plabic graphs were originally introduced by A. Postnikov [22, Section 12], who used them to describe parametrizations of cells in totally nonnegative Grassmannians. A closely related class of graphs was defined by T. Kawamura [14] in the context of the topological theory of *graph divides*. Our definition is very close to Postnikov's.

Remark 7.1.3. In some contexts, it is useful to drop the third condition in Definition 7.1.1 to allow components of G disconnected from the boundary.

Definition 7.1.4. We say that a plabic graph is *leafless* if it has no leaves. (Note that a leafless plabic graph may have lollipops.)

For simplicity, we will mainly restrict our attention to leafless plabic graphs. The results are simpler to state and the proofs are less technical in this setting. Moreover, for most applications of plabic graphs, it suffices to work with leafless plabic graphs. A notable exception is the class of *normal plabic graphs*, which we will study in Section 7.5, and which are in bijection with *triple diagrams*. Normal plabic graphs and triple diagrams will be a key tool in the proof of Theorem 7.1.23.

A key role in the theory of plabic graphs is played by the equivalence relation generated by a family of transformations called (*local*) *moves*.

Definition 7.1.5. We say that two leafless plabic graphs G and G' are *move-equivalent*, and write $G \sim G'$, if G and G' can be related to each other via a sequence of the following *local moves*, denoted (M1), (M2), and (M3):

(M1) (The *square move*) Change the colors of all vertices on the boundary of a quadrilateral face, provided these colors alternate and these vertices are trivalent. See Figure 7.2.

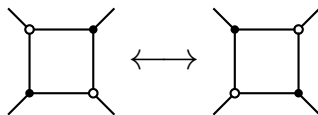


Figure 7.2. Move (M1) on plabic graphs.

(M2) Remove a bivalent vertex (of any color) and merge the edges adjacent to it; or, conversely, insert a bivalent vertex in the middle of an edge. See Figure 7.3.

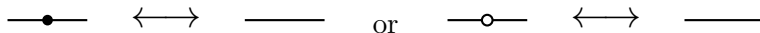


Figure 7.3. Move (M2) on plabic graphs.

(M3) Contract an edge connecting two internal vertices of the same color, as in Figure 7.4; or, conversely, “uncontract” an internal vertex of degree d into two vertices of the same color, joined by an edge, with degrees $d_1 + 1$ and $d_2 + 1$, where $d_1, d_2 > 0$ and $d_1 + d_2 = d$.

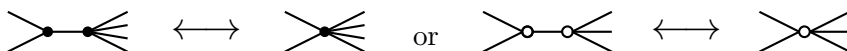


Figure 7.4. Move (M3) on plabic graphs. The number of “hanging” edges on each side must be positive.

Note that if G is bipartite, then the square move (M1) is closely related to the *spider move*, see Definition 2.5.3 as well as Definition 7.5.14 below.

Definition 7.1.6. A leafless plabic graph G is *reduced* if there is no plabic graph $G' \sim G$ such that G' contains a *hollow monogon* or a *hollow digon*, that is, an internal face bounded by one or two edges, see Figure 7.5.

A plabic graph G with leaves is *reduced* if it can be converted into a reduced leafless plabic graph \overline{G} via the following operations:

- (1) contract a leaf edge if both of its endpoints have the same color (note that this is not an (M3) move);
- (2) delete a 2-valent vertex via (M2).

Otherwise we say that G is *non-reduced*.

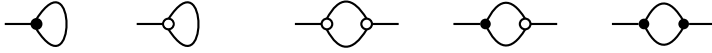


Figure 7.5. A leafless plabic graph is not reduced if and only if it is move-equivalent to a graph containing a hollow monogon or digon.

In this chapter, we will mainly restrict our attention to leafless graphs.

Remark 7.1.7. For a leafless plabic graph, the property of being reduced is invariant under local moves. Note however that this property is not readily testable because it requires understanding all graphs in the move-equivalence class of a plabic graph. We will later obtain several other criteria for testing this property, see Corollary 7.1.25, Theorem 7.8.5, and Theorem 7.11.5.

The most fundamental result concerning reduced plabic graphs is their classification up to move-equivalence (cf. Remark 7.1.7), to be given in Theorem 7.1.23 below. To state this result, we will need some preparation.

Definition 7.1.8. A *trip* τ in a plabic graph G is a walk along the edges of G that either begins and ends at boundary vertices (with all intermediate vertices internal), or is a closed walk entirely contained in the interior of the disk. This walk must obey the following *rules of the road*:

- at a black (respectively, white) vertex of degree at least 2, τ always makes the sharpest possible right (respectively, left) turn onto a different edge;
- at a vertex of degree 1 (e.g., a lollipop), τ makes a U-turn.

Remark 7.1.9. Any walk which starts at a boundary vertex and obeys the rules of the road must necessarily end at a boundary vertex; we call such a trip a *one-way trip*. We refer to a trip which is entirely contained in the interior of the disk as a *roundtrip*.

A one-way trip may begin and end at the same vertex. For example, a trip that starts at a boundary vertex i incident to a lollipop will end at i .

Remark 7.1.10. Just as different countries have different rules regarding which side of the road one should drive on, different authors make conflicting choices for the rules of the road for plabic graphs. In this book, we consistently use the convention chosen in Definition 7.1.8.

Remark 7.1.11. The notion of a trip and the condition of being reduced have appeared in the study of dimer models in statistical mechanics, wherein trips have been called *zigzag paths* [15]. Reduced plabic graphs were called “marginally geometrically consistent” in [4, Section 3.4], and were said to “obey condition Z” in [3, Section 8].

Exercise 7.1.12. Show that one-way trips starting at different vertices terminate at different vertices.

Remark 7.1.13. For any edge e in G and a choice of direction along e , there is a unique trip traversing e in the chosen direction. It may happen that the same trip traverses e twice (once in each direction).

Definition 7.1.14. Let G be a plabic graph with b boundary vertices. The *trip permutation* $\pi_G : \{1, \dots, b\} \rightarrow \{1, \dots, b\}$ is defined by setting $\pi_G(i) = j$ whenever the trip originating at i terminates at j . We will mostly use the one-line notation $\pi_G = (\pi_G(1), \dots, \pi_G(b))$ to represent these permutations.

To illustrate, in Figure 7.1(a), we have $\pi_G = (3, 4, 5, 1, 2)$. Note that Definition 7.1.14 is well-defined because of Exercise 7.1.12.

Exercise 7.1.15. Show that move-equivalent plabic graphs have the same trip permutation.

Remark 7.1.16. The notion of a trip permutation can be further enhanced to construct finer invariants of local moves. For example, we can record, in addition to the trip permutation, the suitably defined *winding number* of each trip. These winding numbers do not change under local moves. A more powerful invariant associates to any plabic graph a particular (transverse) link, see [9].

The following statement will be proved in Section 7.7.

Proposition 7.1.17. *Let G be a reduced leafless plabic graph. If $\pi_G(i) = i$, then the connected component of G containing the boundary vertex i is a lollipop.*

Definition 7.1.18. A *decorated permutation* $\tilde{\pi}$ on b letters is a permutation of the set $\{1, \dots, b\}$ together with a *decoration* of each fixed point by either an overline or an underline. In other words, for every i , we have

$$\tilde{\pi}(i) \in \{\bar{i}, \underline{i}\} \cup \{1, \dots, b\} \setminus \{i\}.$$

An example of a decorated permutation on 6 letters is $(3, 4, 5, 1, 2, \bar{6})$.

Exercise 7.1.19. Show that the number of decorated permutations on b letters is equal to $b! \sum_{k=0}^b \frac{1}{k!}$.

Definition 7.1.20. Let G be a reduced leafless plabic graph. The *decorated trip permutation* π_G associated with G is defined by

$$\tilde{\pi}_G(i) = \begin{cases} \pi_G(i) & \text{if } \pi_G(i) \neq i; \\ \bar{i} & \text{if } G \text{ has a white lollipop at } i; \\ \underline{i} & \text{if } G \text{ has a black lollipop at } i. \end{cases}$$

Remark 7.1.21. If G is a reduced plabic graph with leaves, we can define $\tilde{\pi}_G$ to be $\tilde{\pi}_{\overline{G}}$, where \overline{G} is as in Definition 7.1.6.

Figure 7.6 shows two reduced plabic graphs with the same decorated trip permutation $(3, 4, 5, 1, 2, \bar{6})$.

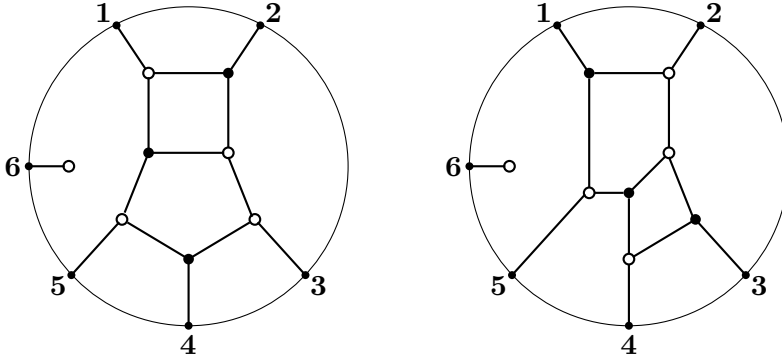


Figure 7.6. Two reduced plabic graphs sharing the same decorated trip permutation $(3, 4, 5, 1, 2, \bar{6})$. Cf. Figure 7.1(b).

Exercise 7.1.15 can be strengthened as follows.

Exercise 7.1.22. The decorated trip permutation of a reduced plabic graph is invariant under local moves.

We will later show (see Corollary 7.10.4) that for each decorated permutation $\tilde{\pi}$ on b letters, there exists a reduced leafless plabic graph whose decorated trip permutation is $\tilde{\pi}$.

Crucially, the move-equivalence class of a reduced plabic graph is completely determined by its decorated trip permutation:

Theorem 7.1.23 (Fundamental theorem of reduced plabic graphs). *Let G and G' be reduced leafless plabic graphs. The following statements are equivalent:*

- (1) G and G' are move-equivalent;
- (2) G and G' have the same decorated trip permutation.

Remark 7.1.24. It is possible to extend Theorem 7.1.23 to the setting of plabic graphs with leaves, using a generalized version of move (M3) that allows the number of hanging edges to be 0. However, the proof is more technical as it needs to deal with “collapsible trees”, see [10].

To illustrate, the two reduced plabic graphs shown in Figure 7.6 have the same decorated trip permutation and consequently are move-equivalent.

We note that the number of faces of a plabic graph is an invariant of its move-equivalence class: that is, the number of faces is preserved under moves (M1), (M2), and (M3). We can use the number of faces and Theorem 7.1.23 to characterize the leafless plabic graphs which are reduced:

Corollary 7.1.25. *Let π be a permutation on b letters. Consider all leafless plabic graphs G whose trip permutation is π ; in particular, G has b boundary vertices. Among all such plabic graphs G , the reduced ones are precisely those that have the smallest number of faces.*

In Corollary 7.10.5, we will give a formula for the number of faces in a reduced plabic graph in terms of the associated decorated trip permutation.

Remark 7.1.26. In Corollary 7.1.25, the requirement that G is leafless cannot be dropped; cf. Figure 7.7.

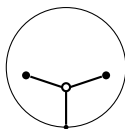


Figure 7.7. This plabic graph G with one boundary vertex has a single face but is not reduced. Note that it is not leafless.

Remark 7.1.27. Some authors call a plabic graph reduced if it has the smallest number of faces among all graphs with a given decorated trip permutation, cf. Corollary 7.1.25. If one adopts this definition, then the graph G in Figure 7.7 becomes reduced. However, there are several reasons that we want to consider this graph to be non-reduced, including the correspondence with triple diagrams, cf. Section 7.7, where we will want reduced plabic graphs to be in bijection with minimal triple diagrams.

Theorem 7.1.23 and Corollary 7.1.25 will be proved in Section 7.7. The statement (1) \Rightarrow (2) in Theorem 7.1.23 is easy, cf. Exercise 7.1.22. The converse implication (2) \Rightarrow (1) is much harder. In Section 7.7, we give a proof of this implication that utilizes D. Thurston’s machinery of triple diagrams, which is presented in Sections 7.5–7.6.

A very intricate argument justifying the implication (2) \Rightarrow (1) was described in Postnikov’s original preprint [22, Section 13]. Another proof of Theorem 7.1.23, involving some difficult results about *plabic tilings* (and relying on Theorem 7.13.4 below), was given by S. Oh and D. Speyer [21].

7.2. Plabic graphs and their quivers

We next associate a quiver to any plabic graph, extending the construction in Definition 2.5.1 to the setting of plabic graphs that need not be bipartite.

Definition 7.2.1. The quiver $Q(G)$ associated to a plabic graph G is defined as follows. The vertices of $Q(G)$ are in one-to-one correspondence with the faces of G . A vertex is mutable (respectively, frozen) if the corresponding face is internal (respectively, incident to the boundary of the disk). For each edge e in G connecting a white vertex to a black vertex and separating two distinct faces, we introduce an arrow connecting the faces separated by e ; this arrow is oriented so that it “sees” the white endpoint of e to the left and the black endpoint to the right as it crosses over e . We then remove oriented 2-cycles from the resulting quiver, one by one, to get $Q(G)$. See Figure 7.8.

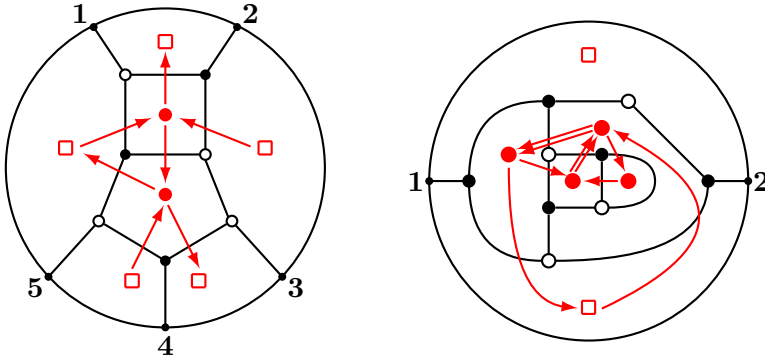


Figure 7.8. Two plabic graphs and their associated quivers. Shown on the left is the graph G from Figure 7.1(a). The quiver on the right has double arrows, corresponding to the instances where a pair of faces share two boundary segments disconnected from each other. The frozen vertex v at the top of the picture is isolated: the two arrows between v and an internal vertex located underneath v cancel each other.

Proposition 7.2.2. Let G and G' be two plabic graphs related to each other by one of the local moves (M1), (M2), or (M3), subject to the restriction that we only allow a square move (M1) at a face F if

(7.2.1) F does not share two consecutive sides with another face;

cf. Figure 7.9. Then the quivers $Q(G)$ and $Q(G')$ are mutation equivalent.

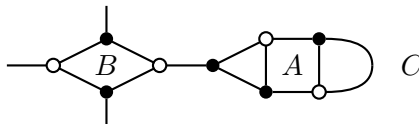


Figure 7.9. Restriction (7.2.1) allows the square move at A —but not at B , since face C is adjacent to two consecutive sides of B .

Proof. It is straightforward to check that a square move in a plabic graph translates into a quiver mutation at the vertex associated to that square face, provided that condition (7.2.1) is satisfied. It is also straightforward to check that the quiver associated with a plabic graph does not change under moves (M2) or (M3), see Figure 7.10. \square

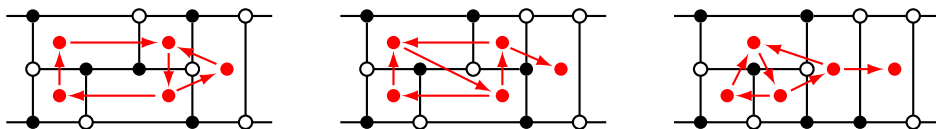


Figure 7.10. Fragments of plabic graphs and their associated quivers. The first two plabic graphs are related by a square move (M1); their quivers are related by a single mutation. The second and the third graphs are related by moves of type (M3), and have isomorphic quivers.

Remark 7.2.3. Suppose that condition (7.2.1) fails at a square face B , with B incident to another face C along two consecutive edges, as in Figure 7.9. Then the arrows transversal to these edges cancel each other, so they do not appear in the associated quiver. This leads to a discrepancy between the square move and the quiver mutation.

Remark 7.2.4. One can always apply a sequence of moves (M2) to a plabic graph to make it bipartite.

Remark 7.2.5. In light of Proposition 7.2.2, one may choose to adjust the definition of the square move (M1)—hence the notion of move-equivalence of plabic graphs—by forbidding square moves violating condition (7.2.1). (This convention was adopted in [9].) We note that for the important subclass of *reduced* plabic graphs (see Definition 7.1.6), condition (7.2.1) is automatically satisfied, so there is no need to worry about it.

Remark 7.2.6. Using Definition 7.2.1, we can associate a seed pattern—hence a cluster algebra—to any plabic graph G . By Proposition 7.2.2, this cluster algebra only depends on the move-equivalence class of G , assuming that we adopt a restricted notion of move-equivalence, cf. Remark 7.2.5. We will soon see that this family of cluster algebras includes all the main examples of cluster algebras (defined by quivers) introduced in the earlier chapters. This justifies the importance of the combinatorial study of plabic graphs, and in particular their classification up to move-equivalence.

The quivers arising from plabic graphs are quite special; in particular, they are planar. Nevertheless, Proposition 7.2.7 below, stated here without proof, shows that quivers from plabic graphs are, in some sense, “universal.”

Proposition 7.2.7 ([8]). *Let Q be a quiver whose vertices are all mutable. Then there exists a plabic graph G such that Q is a full subquiver (see Definition 4.1.1) of a quiver mutation-equivalent to $Q(G)$.*

7.3. Triangulations and wiring diagrams via plabic graphs

In this section, we explain how the machinery of local moves on plabic graphs unifies the combinatorial constructions of Chapter 2, including:

- flips in triangulations of a polygon (Section 2.2);
- braid moves for wiring diagrams (Section 2.3);
- their analogues for double wiring diagrams (Section 2.4).

As mentioned in Remark 7.2.4, the spider move for bipartite graphs (Section 2.5) is equivalent to the square move for plabic graphs.

Example 7.3.1 (Triangulations of a polygon, see [17, Algorithm 12.1]). Let T be a triangulation of a convex m -gon \mathbf{P}_m . The plabic graph $G(T)$ associated to T is constructed as follows:

- (1) Place a white vertex of $G(T)$ at each vertex of \mathbf{P}_m .
- (2) Place a black vertex of $G(T)$ in the interior of each triangle of T . Connect it by edges to the three white vertices of the triangle.
- (3) Embed \mathbf{P}_m into the interior of a disk \mathbf{D} .
- (4) Place m uncolored vertices of $G(T)$ on the boundary of \mathbf{D} .
- (5) Connect each white vertex of $G(T)$ to a boundary vertex. These edges must not cross.

We emphasize that the set of edges of $G(T)$ includes neither the sides of \mathbf{P}_m nor the diagonals of T . See Figure 7.11.

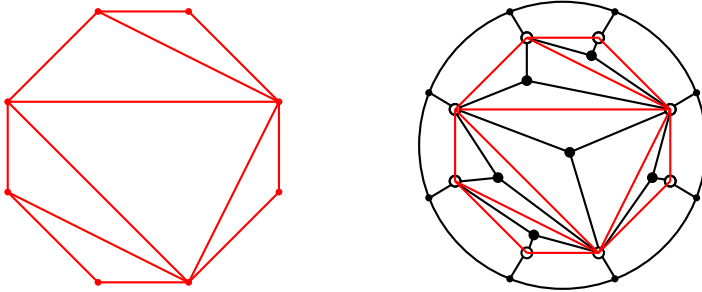


Figure 7.11. A triangulation T of an octagon, and the corresponding plabic graph $G(T)$, cf. Figure 2.2.

Exercise 7.3.2. Show that $Q(G(T)) = Q(T)$, i.e., the quiver associated to the plabic graph of a triangulation T coincides with the quiver $Q(T)$ associated to T , as in Definition 2.2.1.

Exercise 7.3.3. Show that if triangulations T and T' are related by a flip, then the plabic graphs $G(T)$ and $G(T')$ are move-equivalent to each other. More concretely, flipping a diagonal in T translates into a square move at the corresponding quadrilateral face of $G(T)$, plus some (M3) moves to make each vertex of that face trivalent.

Example 7.3.4 (Wiring diagrams). Let D be a wiring diagram, as in Section 1.3. We associate a plabic graph $G(D)$ to D by replacing each crossing in D by a pair of trivalent vertices connected vertically, with a black vertex on top and a white vertex on the bottom. We then enclose the resulting graph in a disk.

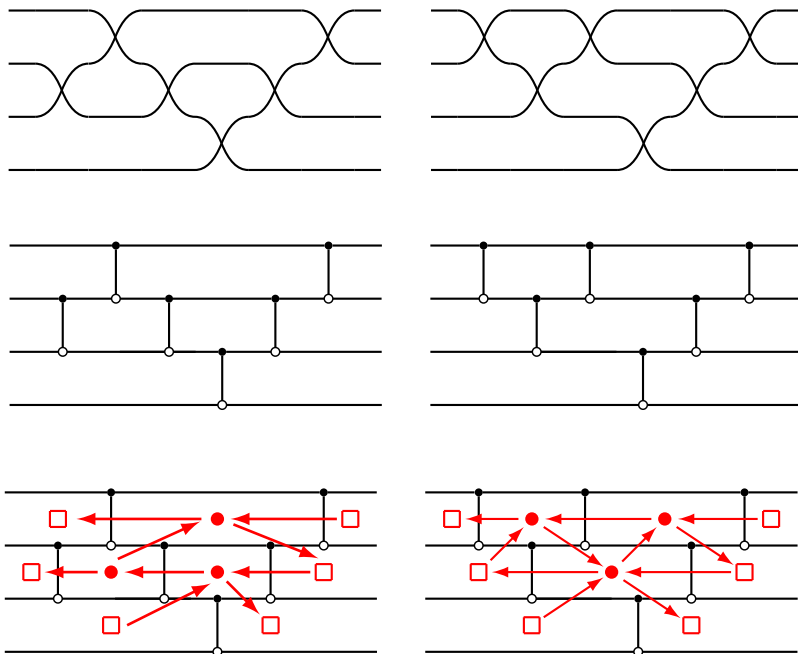


Figure 7.12. Top: wiring diagrams D_1 and D_2 associated to reduced expressions $s_2s_3s_2s_1s_2s_3$ and $s_3s_2s_3s_1s_2s_3$ for $w_0 = (4, 3, 2, 1) \in S_4$. These wiring diagrams (resp., reduced expressions) are related via a braid move. Middle: the plabic graphs $G(D_1)$ and $G(D_2)$. Bottom: the quivers $Q(G(D_1))$ and $Q(G(D_2))$, with isolated frozen vertices removed.

This construction applies to a more general version of wiring diagrams. Let s_i denote the simple transposition in the symmetric group \mathcal{S}_n that exchanges i and $i + 1$. Given a sequence $\mathbf{w} = s_{i_1}s_{i_2}\dots s_{i_m}$ of simple transpositions, we associate to it a diagram $D(\mathbf{w})$ by concatenating m graphs; here the graph associated to s_j consists of n wires, of which $n - 2$ are horizontal, while the j th and $(j + 1)$ st wires cross over each other. See Figure 7.12.

Exercise 7.3.5. Let D be a wiring diagram. Show that the trips starting at the left side of $G(D)$ follow the pattern determined by the strands of D , while the trips starting at the right side of $G(D)$ proceed horizontally to the left.

Exercise 7.3.6. Show that after removing isolated frozen vertices at the top and bottom, the quiver $Q(G(D))$ associated to the plabic graph of a wiring diagram D coincides with the quiver $Q(D)$ associated to D , as in Definition 2.3.1, up to a global reversal of arrows.

Remark 7.3.7. If we changed our convention in Example 7.3.4, swapping the colors of the black and white vertices, we'd recover precisely the quiver $Q(D)$ associated to the wiring diagram. However, we prefer the convention used in Example 7.3.4 because it will lead to a transparent algorithm for recovering the chamber minors, as shown in Figure 7.58. And as noted in Remark 3.1.10, the cluster algebra associated to a given quiver is the same as the cluster algebra associated to the opposite quiver.

Remark 7.3.8. If two wiring diagrams D and D' are related by a braid move, then the corresponding plabic graphs $G(D)$ and $G(D')$ are related by a square move plus some (M3) moves, see Figure 7.13.

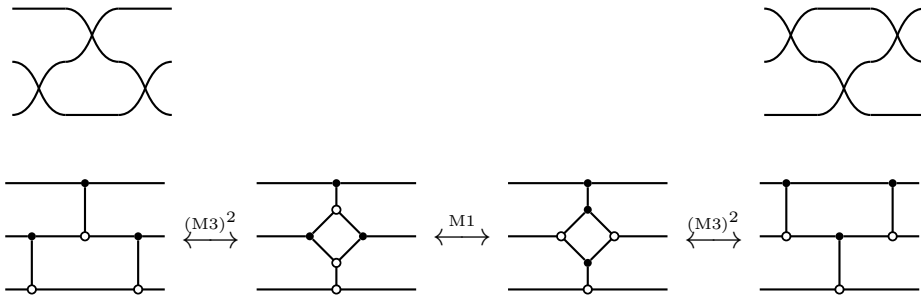


Figure 7.13. A braid move on wiring diagrams, and a corresponding sequence of moves on plabic graphs. The first two (resp., the last two) plabic graphs are related by two (M3) moves; the two plabic graphs in the middle are related by an (M1) move.

Exercise 7.3.9. Consider sequences (or “words”) $\mathbf{w} = s_{i_1} \cdots s_{i_m}$ of simple transpositions in a symmetric group, as in Example 7.3.4. We say that two such words are *braid-equivalent* if they can be related to each other using the braid relations $s_i s_{i+1} s_i = s_{i+1} s_i s_{i+1}$ and $s_i s_j = s_j s_i$ for $|i - j| \geq 2$. A word \mathbf{w} is called a *reduced expression* if no word in its braid equivalence class has two consecutive equal entries: $\cdots s_i s_i \cdots$. Show that if \mathbf{w} fails to be a reduced expression, then $G(D(\mathbf{w}))$ fails to be a reduced plabic graph.

Remark 7.3.10. Conversely, if \mathbf{w} is reduced, then $G(D(\mathbf{w}))$ is reduced; this can be proved using Theorem 7.8.5 or Theorem 7.11.5. In this sense, reduced plabic graphs can be interpreted as generalizations of reduced expressions in symmetric groups.

Example 7.3.11 (Double wiring diagrams). Let D be a double wiring diagram, as in Section 1.4. The plabic graph $G(D)$ associated to D is defined by adjusting the construction of Example 7.3.4 in the following way: as before, we replace each crossing in the double wiring diagram by a pair of trivalent vertices connected vertically, and color one of these vertices white and the other black. If the crossing is thin, the top vertex gets colored white and the bottom one black; if the crossing is thick, the colors of the two vertices are reversed. See Figure 7.14.

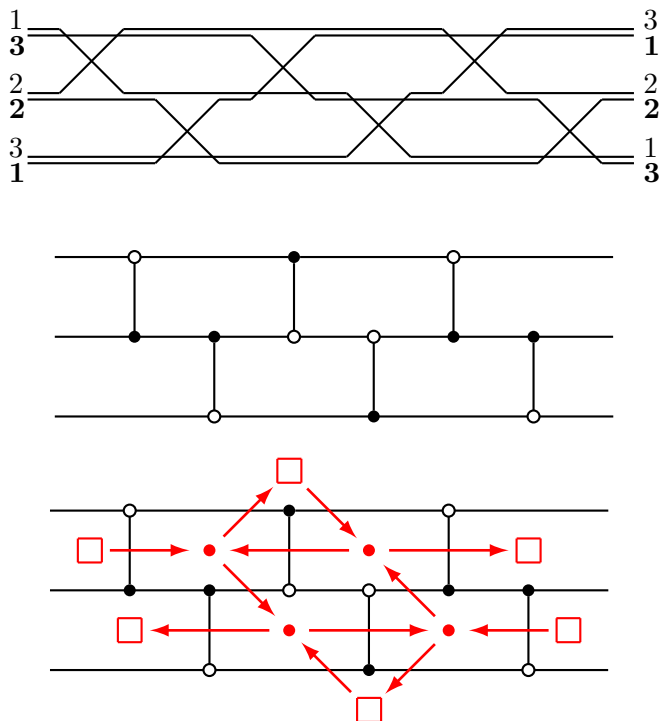


Figure 7.14. A double wiring diagram D , the plabic graph $G(D)$, and the corresponding quiver. If one removes the bottom frozen vertex, one recovers the quiver from Figure 2.6 (up to a global reversal of arrows).

As in Example 7.3.4, the above construction works for a more general version of double wiring diagrams. Given two sequences $\mathbf{w} = s_{i_1}s_{i_2}\dots s_{i_m}$ and $\overline{\mathbf{w}} = \overline{s}_{j_1}\overline{s}_{j_2}\dots \overline{s}_{j_\ell}$, choose an arbitrary shuffle of \mathbf{w} and $\overline{\mathbf{w}}$. Then we can associate a (generalized) double wiring diagram to this shuffle, where thick crossings are associated to factors in \mathbf{w} , and thin crossings are associated to factors in $\overline{\mathbf{w}}$. So, e.g., the double wiring diagram in Figure 7.14 is associated to the shuffle $\overline{s}_2s_1s_2\overline{s}_1\overline{s}_2s_1$.

Exercise 7.3.12. Describe the trips in a plabic graph associated to a double wiring diagram. Extend the statements of Exercise 7.3.6 and Remark 7.3.8 to the case of double wiring diagrams.

In addition to triangulations and wiring diagrams, plabic graphs can also be used to describe Fock-Goncharov cluster structures [7]:

Exercise 7.3.13. Construct a plabic graph whose associated quiver is the quiver shown in Figure 2.3. How does this construction generalize to a quiver $Q_3(T)$ associated to an arbitrary triangulation T of a convex polygon, cf. Exercise 2.2.3?

7.4. Trivalent plabic graphs

In Section 7.2, we introduced plabic graphs and described local moves that generate an equivalence relation on them. In this section, we focus on *trivalent plabic graphs*, i.e., those plabic graphs whose interior vertices are all trivalent. This will require working with an alternative set of moves that preserve the property of being trivalent. As Section 7.4 is not strictly necessary for the sections that follow, it can be skipped if desired.

Remark 7.4.1. Trivalent plabic graphs arise naturally in the studies of

- soliton solutions to the KP equation [17],
- sections of fine zonotopal tilings of 3-dimensional cyclic zonotopes [11],
- combinatorics of planar divides and associated links [9], and
- subdivisions induced by projection of a hypersimplex onto a polygon [23].

Lemma 7.4.2. *Any leafless plabic graph without lollipops can be transformed by a sequence of moves of type (M2) and/or (M3) into a plabic graph all of whose interior vertices are trivalent.*

Proof. We can get rid of bivalent vertices using the moves (M2). If there are any vertices of degree at least 4, split those vertices using (M3) until all internal vertices are trivalent. \square

The alternative set of moves for trivalent plabic graphs consists of the square move (M1) together with the *flip move* (M4) defined below.

Definition 7.4.3. The *flip move* (sometimes also called the *Whitehead move*) for trivalent plabic graphs is defined as follows:

(M4) Replace a fragment containing two trivalent vertices of the same color connected by an edge by another such fragment, see Figure 7.15.

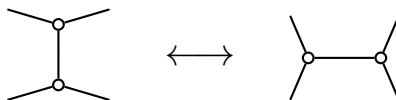


Figure 7.15. The flip move (or Whitehead move) for trivalent graphs. The four vertices shown should either all be white, or all be black.

Remark 7.4.4. A flip move (M4) can be expressed as a composition of two moves of type (M3).

The main result of this section is the following.

Theorem 7.4.5. *Two trivalent plabic graphs are related via a sequence of local moves of types (M1), (M2), and (M3) if and only if they are related by a sequence of moves of types (M1) and (M4).*

The rest of this section is devoted to the proof of Theorem 7.4.5.

Lemma 7.4.6. *If two plabic graphs are related by a sequence of moves of type (M2) and/or (M3), then they are related by moves of type (M3).*

Proof. We first note that in many cases, move (M2) can be thought of as an instance of move (M3): instead of using (M2) to add or remove a bivalent vertex that is adjacent via an edge e to a vertex of the same color, we can use (M3) to (un)contract e , to the same effect.

The only (M2) moves that are genuinely different from (M3) moves are the (M2) moves that add or remove a white (resp., black) vertex in the middle of a black-black or black-boundary (resp., white-white or white-boundary) edge. We call them *creative* or *destructive* (M2) moves, see Figure 7.16. However, if one performs a creative (M2) move, e.g. adding a white vertex in the middle of a black-black or black-boundary edge, there is no further move that the new white vertex can participate in, except for a destructive (M2) move that removes it. Thus, such creative and destructive (M2) moves are unnecessary. \square

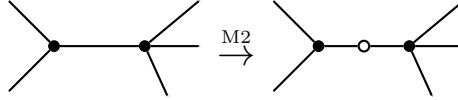


Figure 7.16. A creative (M2) move.

Lemma 7.4.7. *Let G and G' be two trivalent plabic graphs such that*

- *each of the graphs G and G' is connected;*
- *each of the graphs G and G' has f interior faces, b boundary vertices, and b boundary faces (the number of boundary vertices equals the number of boundary faces since the graphs are connected);*
- *in each of the graphs G and G' , all interior vertices have the same color, and this color is the same in both graphs.*

Then G and G' can be connected by a sequence of flip moves (M4).

Proof. The *dual graph* G_{dual} of a trivalent connected plabic graph G is obtained as follows. Place a vertex of G_{dual} in the interior of each face of G . For each edge e of G , introduce a (transversal) edge of G_{dual} connecting the vertices of G_{dual} located in the faces of G on both sides of e , see Figure 7.17. (This new edge may be a loop.) Under the conditions of the lemma, the dual graph G_{dual} is a generalized triangulation T of a (dual) b -gon. (We note that T may contain *self-folded* triangles – loops with an interior “pendant” edge – coming from the faces of G enclosed by a loop in G , as in Figure 7.17.) The triangulation T has $b + f$ vertices: the b vertices of the dual b -gon together with the f interior points (“punctures”).

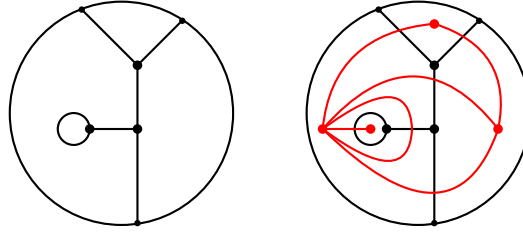


Figure 7.17. A trivalent plabic graph G and its dual graph G_{dual} (in red); the latter contains a self-folded triangle. Here $b = 3$ and $f = 1$.

Figure 7.18 shows that a flip move in a trivalent plabic graph corresponds to a flip in the corresponding triangulation. The claim that G and G' are connected by flip moves can now be obtained from the well-known fact [12, 13] that any two triangulations of a b -gon (including triangulations involving self-folded triangles) with f interior points are connected by flips. \square

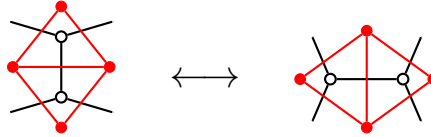


Figure 7.18. The flip move for trivalent graphs corresponds to a flip of the corresponding dual triangulations.

Definition 7.4.8. A *white component* W of a plabic graph G is obtained by taking a maximal (by inclusion) connected induced subgraph of G all of whose internal vertices are white, together with the half-edges extending from the (white) vertices of W towards black vertices outside W or towards boundary vertices of G . *Black components* of G are defined in the same way, with the roles of black and white vertices reversed.

Remark 7.4.9. Each black or white component C of a plabic graph G can itself be regarded as a (generalized) plabic graph. To this end, enclose C by a simple closed curve γ passing through the endpoints of the half-edges on the outer boundary of C . If the portion of G located inside γ is exactly C , then we get a usual plabic graph. It may however happen that C contains “holes,” i.e., some of the half-edges on the boundary of C may be entirely contained in the interior of the disk enclosed by γ . In that case, we need to draw simple closed curves through the endpoints of those half-edges, so that C becomes a generalized plabic graph inside a “swiss-cheese” shape (a disk with some smaller disks removed), as in Figure 7.19. The argument in the proof of Lemma 7.4.7 extends to this setting, so Lemma 7.4.7 also holds for black/white components of trivalent plabic graphs. We will use this generalization in the proof of Proposition 7.4.10 below.

Proposition 7.4.10. *If two trivalent plabic graphs are related to each other by moves (M2) and/or (M3), then they are related via flip moves (M4).*

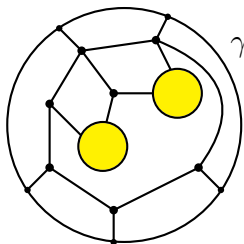


Figure 7.19. A generalized plabic graph inside a “swiss-cheese” shape (in this case, a disk with two smaller disks removed).

Proof. Without loss of generality, we assume that the given plabic graphs G, G' are connected. By Lemma 7.4.6, they are related by moves (M3).

Each of the graphs G and G' breaks into disjoint (white or black) components. Each (M3) move only affects a single component. It follows that the white (resp., black) components W_1, \dots, W_ℓ (resp., B_1, \dots, B_m) of G are in bijection with the components W'_1, \dots, W'_ℓ (resp., B'_1, \dots, B'_m) of G' , so that each W_i (resp., B_j) is related to W'_i (resp., B'_j) via (M3) moves.

Since an (M3) move preserves the number of boundary vertices and the number of faces, both W_i and W'_i (respectively, B_j and B'_j) have the same number of boundary vertices and the same number of faces. It now follows from Lemma 7.4.7 (more precisely, from its extension to components of plabic graphs, see Remark 7.4.9) that each pair W_i and W'_i can be connected by flip moves, and similarly for B_j and B'_j . The proposition follows. \square

Proof of Theorem 7.4.5. The “if” direction follows from Remark 7.4.4.

Suppose that G and G' are related via a sequence of (M1), (M2), and (M3) moves. Let k denote the number of square moves (M1) in the sequence. We then have a sequence of move-equivalences

$$G = G'_0 \sim G_1 \sim G'_1 \sim G_2 \sim G'_2 \sim \dots \sim G_k \sim G'_k \sim G_{k+1} = G',$$

where for all i , G_i is related to G'_i by a single square move, whereas G'_i is related to G_{i+1} by a sequence of (M2) and (M3) moves. Since a square move only involves trivalent vertices, we may assume, applying extra (M2) and (M3) moves as needed, that all plabic graphs G_i and G'_i are trivalent. It then follows by Proposition 7.4.10 that for every i , the graphs G'_i and G_{i+1} are related by flip moves alone, and we are done. \square

Remark 7.4.11. Plabic graphs associated to wiring diagrams (ordinary or double), cf. Examples 7.3.4 and 7.3.11, are trivalent. Consequently, one can express the transformations corresponding to braid moves using square moves and flip moves, as shown in Figure 7.13. On the other hand, plabic graphs associated to triangulations of a polygon (see Example 7.3.1 and Figure 7.11) are *not* trivalent.

7.5. Triple diagrams and normal plabic graphs

Triple diagrams (or triple crossing diagrams), introduced by D. Thurston in [25], are planar topological gadgets closely related to plabic graphs. Our treatment of triple diagrams in Sections 7.5–7.6 is largely based on [25].

Definition 7.5.1. Let \mathfrak{X} be a collection of oriented closed intervals and oriented circles immersed into a closed disk \mathbf{D} . The image of each interval I or circle C is called a *strand*; it inherits its orientation from I or C . The strands that are immersed intervals (resp., circles) are called *arcs* (resp., *closed strands*). A *face* of \mathfrak{X} is a connected component of the complement of the union of all strands within \mathbf{D} . We call \mathfrak{X} a *triple diagram* if

- the endpoints of arcs are distinct points located on the boundary $\partial\mathbf{D}$; each arc meets the boundary transversally;
- each closed strand is entirely contained in the interior of \mathbf{D} ;
- every point that lies on more than one local branch of a strand is a *triple point* in the interior of \mathbf{D} where exactly three local branches meet, intersecting each other transversally;
- the union of the strands and the boundary $\partial\mathbf{D}$ is connected; this ensures that each face is homeomorphic to an open disk;
- the strand segments lying on the boundary of each face are oriented consistently (i.e., clockwise or counterclockwise); in particular, as we move along the boundary, the *sources* (endpoints where an arc runs away from $\partial\mathbf{D}$) alternate with the *targets* (where an arc runs into $\partial\mathbf{D}$).

Each triple diagram, say with b arcs, comes with a selection of b distinguished points on $\partial\mathbf{D}$ that are called *boundary vertices*. There is one such boundary vertex within every other segment of $\partial\mathbf{D}$ between two consecutive arc endpoints. Specifically, we place boundary vertices so that, moving clockwise along the boundary, each boundary vertex follows (resp., precedes) a source (resp., a target). We label the boundary vertices $1, \dots, b$ in clockwise order. See Figure 7.20.

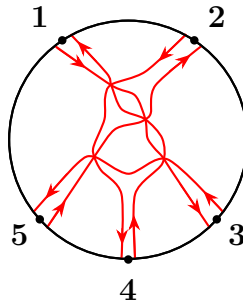


Figure 7.20. A triple diagram \mathfrak{X} with the strand permutation $\pi_{\mathfrak{X}} = (3, 4, 5, 1, 2)$.

Triple diagrams are viewed up to smooth isotopy among such diagrams. This makes them essentially combinatorial objects: 6-valent/univalent directed graphs with some additional structure.

Remark 7.5.2. In [25], the definition of a triple diagram does not include the restriction appearing in Definition 7.5.1 that requires the union of the strands and the boundary $\partial \mathbf{D}$ to be connected. In the terminology of [25], all our triple diagrams are *connected*.

Remark 7.5.3. In order to ensure consistent orientations along the face boundaries, the orientations of strands must alternate between “in” and “out” around each triple point. Given a triple diagram with unoriented strands, we can satisfy this condition as follows: start anywhere and propagate out by assigning alternating orientations around vertices.

Definition 7.5.4. Let \mathfrak{X} be a triple diagram with b boundary vertices (hence b arcs). For each boundary vertex i , let s_i (resp., t_i) denote the source (resp., target) arc endpoint located next to i on the boundary of \mathbf{D} .

The *strand permutation* $\pi_{\mathfrak{X}}$ is defined by setting $\pi_{\mathfrak{X}}(i) = j$ whenever the arc originating at s_i ends up at t_j . Thus, the strand permutation describes the connectivity of the arcs. See Figure 7.20.

We will soon see (cf. Definition 7.6.8 below) that any permutation can arise as a strand permutation of a triple diagram.

Just as the local moves on plabic graphs preserve the (decorated) trip permutation (see Exercise 7.1.22), there is a notion of a local move on triple diagrams that keeps the strand permutation invariant.

Definition 7.5.5. A *swivel move* is a local transformation of triple diagrams that is shown in Figure 7.21. (This move is called a $2 \leftrightarrow 2$ move in [25].) We say that two triple diagrams \mathfrak{X} and \mathfrak{X}' are *move-equivalent* to each other, and write $\mathfrak{X} \sim \mathfrak{X}'$, if one can get from \mathfrak{X} to \mathfrak{X}' via a sequence of swivel moves.

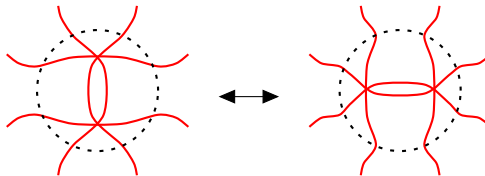


Figure 7.21. The swivel move replaces one of these fragments of a triple diagram by the other fragment, then smoothens out the strands. The orientation of each strand on the left should match the orientation of the strand on the right that has the same endpoints.

Remark 7.5.6. The connectivity of strands on both sides of Figure 7.21 is the same, so the strand permutation is invariant under the swivel move.

We will soon see that triple diagrams are cryptomorphic to a variant of plabic graphs that we call *normal plabic graphs*, defined below.

Definition 7.5.7. Let G be a plabic graph, where we allow leaves. We say that G is *normal* if the coloring of its internal vertices is bipartite, all white vertices in G are trivalent, and each boundary vertex is adjacent to a black vertex. See Figure 7.22.

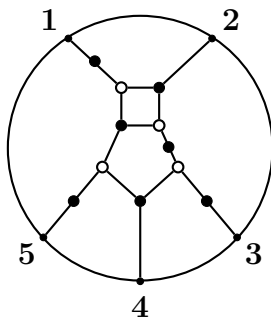


Figure 7.22. A normal plabic graph G . This graph was obtained from the one in Figure 7.1(a) by inserting several bivalent black vertices.

Remark 7.5.8. If a normal plabic graph G has a leaf or a lollipop, it must be black, since white vertices are required to be trivalent. Therefore, in the case of normal graphs, there is no need to decorate the trip permutation.

Remark 7.5.9. If a normal plabic graph G has a black leaf, then G will fail to be reduced, see Definition 7.1.6.

Definition 7.5.10 below associates a diagram $\mathfrak{X}(G)$ to a normal plabic graph. We will then show in Lemma 7.5.11 that $\mathfrak{X}(G)$ is indeed a triple diagram.

Definition 7.5.10. Given a normal plabic graph G , we associate a diagram $\mathfrak{X}(G)$ as follows. To each trip in G —either a one-way trip or a roundtrip—we associate a strand in the ambient disk \mathbf{D} by slightly deforming the trip, as shown in Figure 7.23, so that the strand

- runs along each edge of the trip, keeping the edge on its left,
- makes a U-turn at each black internal leaf (a vertex of degree 1),
- ignores black vertices of degree 2,
- makes a right turn (as sharp as possible) at each other black vertex, and
- makes a left turn at each white vertex v along the trip, passing through v .

See Figure 7.24 for an example.

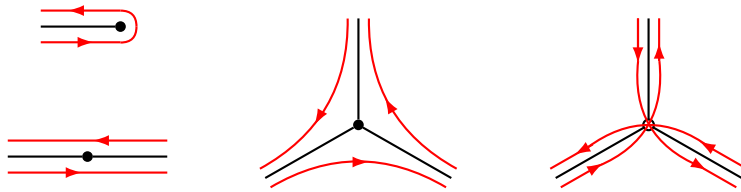


Figure 7.23. Constructing a triple diagram from a normal plabic graph.

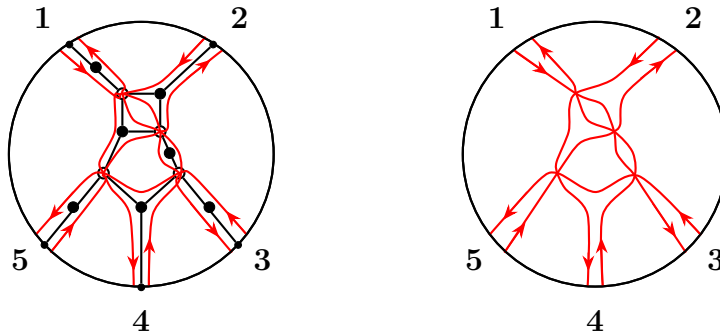


Figure 7.24. Left: A normal plabic graph G (cf. Figure 7.22) together with the associated triple diagram $\mathfrak{X} = \mathfrak{X}(G)$. Conversely, $G = G(\mathfrak{X})$. Right: The triple diagram $\mathfrak{X} = \mathfrak{X}(G)$. The trip permutation of G and the strand permutation of \mathfrak{X} are equal: $\pi_G = \pi_{\mathfrak{X}} = (3, 4, 5, 1, 2)$.

Lemma 7.5.11. *The diagram $\mathfrak{X}(G)$ associated to a normal plabic graph G as in Definition 7.5.10 is a triple diagram.*

Proof. Since the white vertices in G are trivalent, $\mathfrak{X}(G)$ has a triple point for every white vertex in G , and no other crossings. We need to check that $\mathfrak{X} = \mathfrak{X}(G)$ is connected, or more precisely, that the union of the strands and the boundary of the disk is connected, as required by Definition 7.5.1.

Let us ignore any component consisting of a single black vertex which is adjacent only to boundary vertices (e.g. a black lollipop), as the corresponding strands are clearly connected to the boundary of the disk. Consider any other strand S in \mathfrak{X} . By construction, S passes through at least one white vertex of the (bipartite) graph G , which is a triple point on S . It therefore suffices to show that every triple point in \mathfrak{X} is connected to the boundary within \mathfrak{X} (i.e., via strand segments of \mathfrak{X}).

Let u be a k -valent black vertex in G and let v_1, \dots, v_k be the white or boundary vertices adjacent to u . The strands of \mathfrak{X} that run along the k edges of G incident to u cyclically connect the triple points v_1, \dots, v_k to each other. (If the list v_1, \dots, v_k includes boundary vertices, then the corresponding strand segments are connected via the boundary.) We conclude that for any two-edge path $v - u - v'$ in G connecting two white or boundary vertices

v and v' via a black vertex u , the triple (or nearby boundary) points v and v' are connected within \mathfrak{X} . It follows that for any path in the bipartite graph G connecting a white vertex v to the boundary, there is a path in \mathfrak{X} that connects the triple point v to the boundary.

It remains to note that by Definition 7.1.1, any white vertex v in G is connected by a path in G to some boundary vertex. \square

We now go in the opposite direction, from a triple diagram to a normal plabic graph.

Definition 7.5.12. The normal plabic graph $G = G(\mathfrak{X})$ associated to a triple diagram \mathfrak{X} is constructed as follows. Place a white vertex of G at each triple crossing in \mathfrak{X} . Treat each boundary vertex of \mathfrak{X} as a boundary vertex of G . For each region R of \mathfrak{X} whose boundary is oriented counterclockwise, place a black vertex in the interior of R and connect it to the white and boundary vertices lying on the boundary of R , so that each white (resp., boundary) vertex is trivalent (resp., univalent). The resulting plabic graph $G = G(\mathfrak{X})$ is normal by construction.

Proposition 7.5.13. The maps $G \mapsto \mathfrak{X}(G)$ and $\mathfrak{X} \mapsto G(\mathfrak{X})$ described in Definitions 7.5.10 and 7.5.12 are mutually inverse bijections between normal plabic graphs and triple diagrams with the same number of boundary vertices. The trip permutation π_G of a normal graph G is equal to the strand permutation $\pi_{\mathfrak{X}}$ of the corresponding triple diagram $\mathfrak{X} = \mathfrak{X}(G)$.

Figure 7.25 illustrates the bijection between normal plabic graphs and triple diagrams in the case of reduced normal plabic graphs on three nodes.

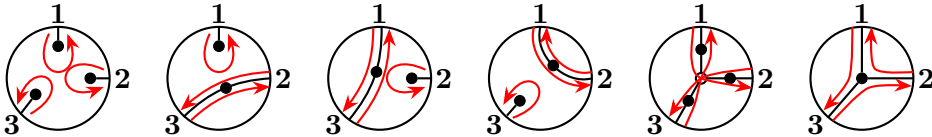


Figure 7.25. The six reduced normal plabic graphs with three boundary vertices, shown together with the corresponding triple diagrams, cf. Definition 7.5.10. The associated trip (resp., strand) permutations are precisely the six permutations of $\{1, 2, 3\}$.

Proof. Starting from a normal graph G , let us decompose it into star-shaped subgraphs S_v each of which includes a black vertex v , all the edges incident to v , and the endpoints of those edges. Each of these stars will give rise to a fragment of the triple diagram $\mathfrak{X}(G)$ that “hugs” the edges of S_v and whose boundary is oriented counterclockwise (looking from v). Moreover, $\mathfrak{X}(G)$ is obtained by stitching these fragments together. Applying the map $\mathfrak{X} \mapsto G(\mathfrak{X})$ to $\mathfrak{X}(G)$ will recover the original graph G .

One similarly shows that if we start from a triple diagram \mathfrak{X} , construct the normal graph $G(\mathfrak{X})$, and then apply the map $G \mapsto \mathfrak{X}(G)$ to $G(\mathfrak{X})$, then we recover the original triple diagram \mathfrak{X} . The key property to keep in mind is that each face of \mathfrak{X} is homeomorphic to an open disk.

The strands of \mathfrak{X} run alongside the trips of G , implying that $\pi_{\mathfrak{X}} = \pi_G$. \square

In Theorem 7.7.1, we will characterize triple diagrams that correspond, under the bijection of Proposition 7.5.13, to *reduced* normal plabic graphs.

The bijective correspondence between triple diagrams and normal plabic graphs can be used to translate the equivalence of triple diagrams under swivel moves, cf. Definition 7.5.5, into a variant of move equivalence of plabic graphs (cf. Definition 7.1.5) adapted to the setting of normal plabic graphs:

Definition 7.5.14. The (*normal*) *spider move* is a local transformation of a normal plabic graph G that replaces one of the fragments shown in Figure 7.26 (see also Figure 7.27) by the other. To be more precise, assume that G contains a quadrilateral face with black vertices A, A' and white vertices K, K' . Let K (resp., K') be adjacent to the black vertices A, A', B (resp., A, A', B'). We then replace the white vertices K, K' (resp., the 6 edges adjacent to them) by the new white vertices L, L' (resp., the edges $AL, BL, B'L, A'L', BL', B'L'$).

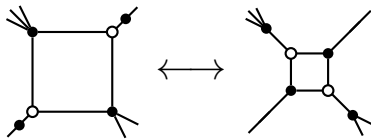


Figure 7.26. A normal spider move.

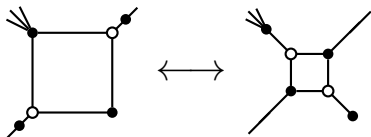


Figure 7.27. A normal spider move for a quadrilateral face incident to a bivalent vertex. By Remark 7.5.9, this may only occur for non-reduced normal plabic graphs.

Remark 7.5.15. The normal spider moves introduced in Definition 7.5.14 are slightly different from the square moves described in Figure 7.2 (resp., Definition 2.5.3), which required each vertex of the quadrilateral face to have degree 3 (resp., degree at least 3).

Definition 7.5.16. The *normal flip move* is the local transformation shown in Figure 7.28. Ignoring the bivalent black vertices, this local move is the same as the (white) flip move for trivalent plabic graphs.

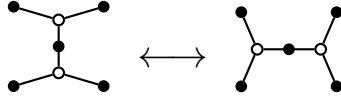


Figure 7.28. The normal flip move.

We want to relate the normal spider move and the normal flip move to the moves (M1), (M2), (M3) that we saw in Section 7.1. In order to do so, we need the following variant of (M3).

Definition 7.5.17. The move (M3') on plabic graphs contracts or uncontracts two internal vertices of the same color, and is defined as in Figure 7.4, except that if both vertices are black, then the number of “hanging” edges on either side can be any *nonnegative* integer. In particular, (M3') can create or remove a black leaf.

Definition 7.5.18. Let G and G' be plabic graphs. We write $G \stackrel{\bullet}{\sim} G'$ if G and G' can be related to each other via local moves (M1), (M2), and/or (M3').

Lemma 7.5.19. *Let G and G' be normal plabic graphs related via a sequence of normal spider moves and normal flip moves. Then $G \stackrel{\bullet}{\sim} G'$.*

Proof. Degenerate versions of the normal spider move, as in Figure 7.27, can be expressed as a square move (M1) together with (M2) and/or (M3') moves. Nondegenerate versions of the normal spider move, as well as the normal flip move, can be expressed as a combination of (M1), (M2) and (M3) moves. (In particular, (M3') is not needed for these.) \square

By Remark 7.5.9 and Definition 7.1.6, a normal plabic graph which is reduced must be leafless.

Lemma 7.5.20. *Let G and G' be normal plabic graphs which are reduced, and which are related via a sequence of normal spider moves and normal flip moves. Then $G \sim G'$.*

Proof. Since G and G' are reduced, we will never need to use a degenerate spider move to relate them to each other. Both the nondegenerate normal spider move and the normal flip move can be expressed in terms of (M1), (M2), and (M3). \square

Theorem 7.5.21. *Let G and G' be normal plabic graphs and let $\mathfrak{X} = \mathfrak{X}(G)$ and $\mathfrak{X}' = \mathfrak{X}(G')$ be the corresponding triple diagrams. Then the following are equivalent:*

- G and G' are related via a sequence of normal spider moves and/or normal flip moves;
- \mathfrak{X} and \mathfrak{X}' are move-equivalent (i.e., related via swivel moves).

Proof. Figure 7.29 shows that each swivel move in a triple diagram $\mathfrak{X}(G)$ corresponds to—depending on the orientations of the strands—either a normal spider move or a normal flip move in the normal plabic graph G . The statement of the theorem follows. \square

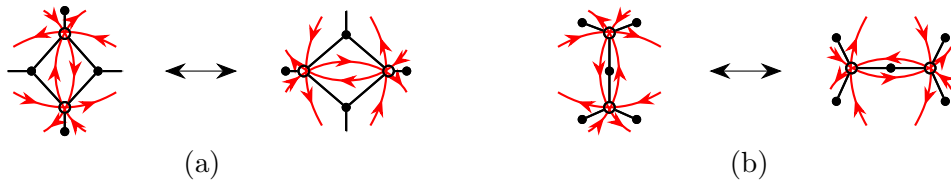


Figure 7.29. Depending on the orientations of the strands involved, a swivel move in a triple diagram may correspond to (a) a normal spider move or (b) a normal flip move in the associated normal plabic graph.

Our next goal is to give an analogue of Definition 7.5.10 for arbitrary leafless plabic graphs, not necessarily normal.

Definition 7.5.22. Let G be a (leafless) plabic graph, not necessarily normal. The *normal form* associated to G , is a (non-unique) plabic graph $N(G)$ which is move-equivalent to G , constructed as follows (see Figure 7.30).

- Use (M2) to omit degree 2 white vertices.
- Use (M3) to contract all edges with both endpoints black. (If this results in a loop, then the graph is not reduced.)
- Use (M3) to turn white vertices of degree ≥ 4 into subgraphs whose vertices are white and trivalent.
- Use (M2) to add degree 2 black vertices so that that the resulting graph is bipartite and each boundary vertex is adjacent to a black vertex.

Note that if G is reduced and has no white lollipops, then $N(G)$ is normal.

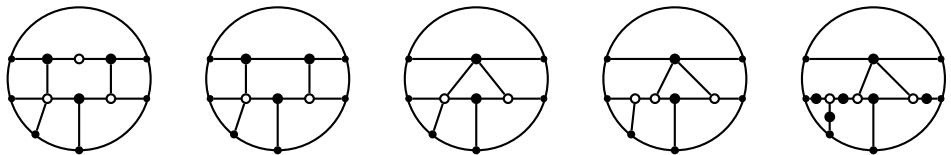


Figure 7.30. A reduced plabic graph G (left) and a normal form $N(G)$ (right).

Now we define the *generalized triple diagram* $\mathfrak{X}(G) = \mathfrak{X}(N(G))$ associated to G by applying Definition 7.5.10 to the normal form $N(G)$, with the following additional rule dealing with white lollipops:

- at a white lollipop in G , make a U-turn:

Remark 7.5.23. Given G , there are many possible choices for $N(G)$, since the trivalent tree replacing v is not unique. Nevertheless, all these trees are related to each other by flip moves, cf. Figure 7.15. Hence all triple diagrams constructed from them are move-equivalent to each other, cf. Figure 7.29(b) (remove the black vertex in the center).

The following statement is immediate from the definitions.

Lemma 7.5.24. *Let G be a plabic graph. If the union of the strands in $\mathfrak{X}(G)$ and the boundary $\partial \mathbf{D}$ is connected, then $\mathfrak{X}(G)$ is a triple diagram in the sense of Definition 7.5.1.*

The connectedness condition in Lemma 7.5.24 does not hold in general. To be concrete, if G contains a cycle C all of whose vertices are black, then the strands located inside C are disconnected from the rest of $\mathfrak{X}(G)$.

Lemma 7.5.25. *Let G and G' be (leafless) plabic graphs such that $G \stackrel{\bullet}{\sim} G'$. Then the corresponding (generalized) triple diagrams $\mathfrak{X}(G)$ and $\mathfrak{X}(G')$ are move-equivalent (i.e., related to each other via swivel moves).*

We note that $\mathfrak{X}(G)$ and $\mathfrak{X}(G')$ are defined up to move-equivalence, so the statement that they are move-equivalent to each other makes sense.

Proof. It is straightforward to verify, case by case, that each of the local moves (M1)–(M3') either leaves the associated (generalized) triple diagram intact or applies a swivel move to it (more precisely, to any of the possible diagrams obtained via the construction in Definition 7.5.22). To be specific:

- a square move (M1) translates into a swivel move, see Figure 7.29(a);
- both the move (M2) and a black (de)contraction move (M3') leave the triple diagram invariant (up to isotopy);
- a white (de)contraction move (M3') translates into a swivel move, see Figure 7.29(b) (remove the black vertex in the center). \square

Corollary 7.5.26. *Let G and G' be normal plabic graphs. The following are equivalent:*

- (1) $G \stackrel{\bullet}{\sim} G'$;
- (2) G and G' are related via a sequence of normal spider moves and normal flip moves;
- (3) $\mathfrak{X}(G)$ and $\mathfrak{X}(G')$ are move-equivalent (in the sense of Definition 7.5.5).

Proof. The implication (2) \Rightarrow (1) is Lemma 7.5.19. The equivalence (2) \Leftrightarrow (3) was established in Theorem 7.5.21. The implication (1) \Rightarrow (3) was proved in Lemma 7.5.25. \square

We note the similarity between Corollary 7.5.26 and Theorem 7.4.5.

7.6. Minimal triple diagrams

Definition 7.6.1. A triple diagram is called *minimal* if it has no more triple points than any other triple diagram with the same strand permutation.

We will show in Section 7.7 that minimal triple diagrams are the natural counterparts of reduced normal plabic graphs.

Much of this section is devoted to the proof of the following key result.

Theorem 7.6.2. *Any two minimal triple diagrams with the same strand permutation are move-equivalent to each other.*

Lemma 7.6.3. *If a triple diagram \mathfrak{X} is minimal, then so is every triple diagram move-equivalent to \mathfrak{X} .*

Proof. It is easy to see that a swivel move preserves both the number of triple points and the strand permutation. The claim follows. \square

We next describe certain “bad features” (of a triple diagram) and show that they cannot occur in a minimal triple diagram.

Definition 7.6.4. A strand in a triple diagram that intersects itself forms a *monogon*. A pair of strands that intersect at two points x and y form either a *parallel digon* or *anti-parallel digon*, depending on whether their segments connecting x and y run in the same or opposite direction, see Figure 7.31. We use the term *badgon* to refer to either a monogon or a parallel digon.

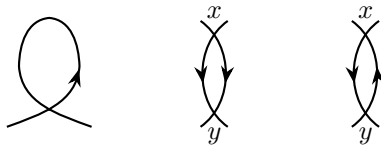


Figure 7.31. A monogon, a parallel digon, and an anti-parallel digon. The actual picture will contain additional strands and intersections.

Lemma 7.6.5. *A triple diagram without badgons has no closed strands.*

Proof. Let \mathfrak{X} be a triple diagram without badgons. Since \mathfrak{X} does not contain monogons, no strand of \mathfrak{X} can intersect itself. Suppose that \mathfrak{X} contains a closed strand S . Let T be another strand of \mathfrak{X} intersecting S at points x and y ; such T exists since \mathfrak{X} must be connected to the boundary $\partial\mathbf{D}$. Then the segment of T between x and y together with one of the segments of S connecting x and y form a parallel digon, which is a contradiction. \square

Lemma 7.6.6. *A minimal triple diagram does not contain badgons. Therefore (cf. Lemma 7.6.5) it does not contain closed strands.*

Proof. Let \mathfrak{X} be a triple diagram containing a monogon, i.e., a strand S with a self-intersection at a triple point v . Construct the triple diagram \mathfrak{X}' by deforming \mathfrak{X} around v so that S “spins off” a closed strand while the triple point disappears, see Figure 7.32. (If the spun-off portion is disconnected from the rest of \mathfrak{X} , then remove it altogether.) The triple diagram \mathfrak{X}' has the same strand permutation as \mathfrak{X} but fewer triple points; thus \mathfrak{X} is not minimal.

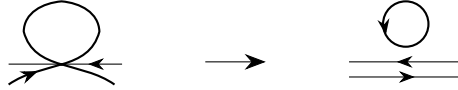


Figure 7.32. In the presence of a monogon, we can reduce the number of triple points while keeping the same strand permutation. The triple diagram may contain additional strands intersecting the monogon, as well as additional points of self-intersection.

Now suppose that \mathfrak{X} does not contain monogons but does contain two strands S and T that form a parallel digon. Say, S and T contain segments \overline{S} and \overline{T} that run from a triple point x to a triple point y . Let U (resp., V) be the third strand passing through x (resp., y). We then deform \mathfrak{X} around both x and y by smoothing each of the two triple points: the strands U and V continue to go straight through, whereas the endpoints of \overline{S} (resp., \overline{T}) get connected to T (resp., S). Thus, the strands S and T swap their segments \overline{S} and \overline{T} with each other (with appropriate smoothings), the overall connectivity (i.e., the strand permutation) is preserved, and the triple points at x and y disappear. (If the diagram becomes disconnected from $\partial\mathbf{D}$, then remove the disconnected portion.) We then conclude that \mathfrak{X} was not minimal. \square

Definition 7.6.7. Let S be an arc in a triple diagram; its endpoints s and t lie on the boundary of the ambient disk \mathbf{D} . We call S *boundary-parallel* if it runs along a segment I of the boundary $\partial\mathbf{D}$ between s and t (in either direction), so that every other strand with an endpoint inside I runs directly to or from S , without any triple crossings in between. See Figure 7.33.

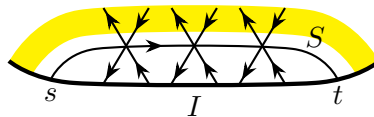


Figure 7.33. A boundary-parallel strand S in a triple diagram.

We next describe a particular way to construct, for any given permutation π , a triple diagram whose strand permutation is π .

Definition 7.6.8. Let π be a permutation of b letters $1, \dots, b$. A triple diagram in the disk \mathbf{D} is called *standard* (for π) if it can be constructed using the following recursive process. (The process involves some choices, so a standard diagram for π is not unique.)

We place b boundary vertices on the boundary $\partial\mathbf{D}$ and label them $1, \dots, b$ clockwise. Next to each boundary vertex v , we mark two endpoints of the future strands: a source endpoint that precedes v in the clockwise order and a target endpoint that follows v in this order. We know which source is to be matched to which target by the strand permutation π . The source and target of a given strand divides the circle $\partial\mathbf{D}$ into two intervals. Let us partially order these $2b$ intervals by inclusion and select a *minimal interval* I with respect to this partial order.

We start constructing the triple diagram by running a boundary-parallel strand S along the interval I , introducing a triple crossing for each pair of strands that need to terminate in the interior of I , as shown in Figure 7.33. There will always be an even number (possibly zero) of strands to cross over, so the construction will proceed without a hitch.

Let \mathbf{D}' be the disk obtained from \mathbf{D} by removing the region between the boundary segment I and the strand S together with a small neighborhood of S ; so \mathbf{D}' is the shaded region in Figure 7.33. We accordingly remove S and its endpoints from the original pairing of the in- and out-endpoints, and swap each pair that S crossed over. This yields $2(b-1)$ endpoints on the boundary of \mathbf{D}' ; note that the in- and out-endpoints alternate, as before. We then determine the new pairing of these endpoints (thus, a new strand permutation, after an appropriate renumbering) and recursively continue the process in \mathbf{D}' until the desired (standard) triple diagram is constructed. See Figure 7.34.

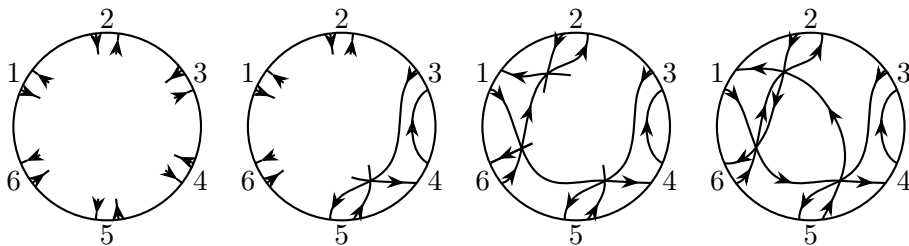


Figure 7.34. Constructing a standard triple diagram associated to the permutation $\pi = (4, 6, 5, 3, 1, 2)$. The figure shows the stages in the construction after: adding boundary-parallel strands $4 \rightarrow 3$ and $3 \rightarrow 5$; then $1 \rightarrow 4$ and $6 \rightarrow 2$; then $2 \rightarrow 6$ and $5 \rightarrow 1$.

We shall keep in mind that a standard triple diagram is constructed by choosing a sequence of minimal intervals.

Exercise 7.6.9. For each of the three pairs of triple diagrams shown in Figure 7.35, demonstrate that the two diagrams are move-equivalent to each other, i.e., are related via a sequence of swivel moves. (In each of the three cases, the central section can involve an arbitrary number of repetitions.)

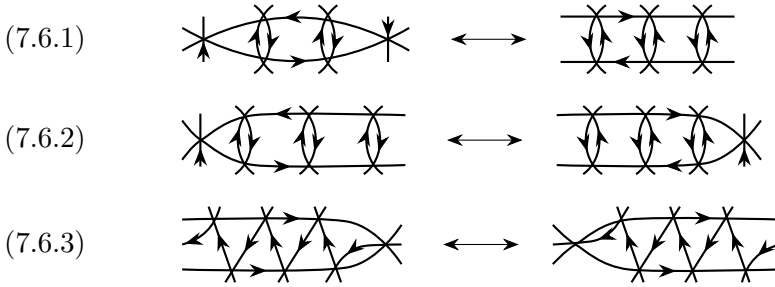
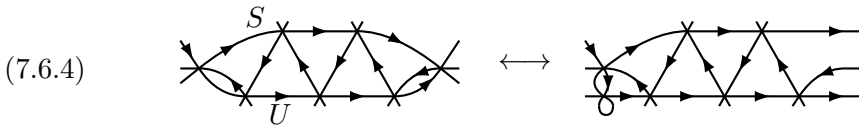


Figure 7.35. Move equivalence of triple diagrams.

Exercise 7.6.10. Use (7.6.3) to prove the move-equivalence (7.6.4) below:



Lemma 7.6.11. *Let \mathfrak{X} be a triple diagram such that no triple diagram move-equivalent to \mathfrak{X} contains a monogon. Then the following statements hold:*

- (i) *No triple diagram move-equivalent to \mathfrak{X} has a badgon or a closed strand.*
- (ii) *Let I be a minimal interval for the strand permutation associated with \mathfrak{X} . Then \mathfrak{X} is move-equivalent to a diagram \mathfrak{X}' in which the strand connecting the endpoints of I is boundary-parallel along I .*

Proof. We will simultaneously prove statements (i) and (ii) by induction on the number of triple points in \mathfrak{X} . Thus, we assume that both (i) and (ii) hold for triple diagrams that have fewer triple points than \mathfrak{X} .

We first prove (i). Suppose that a triple diagram $\mathfrak{X}' \sim \mathfrak{X}$ contains (non-self-intersecting) strands S and U forming a parallel digon. The strand S cuts the disk \mathbf{D} into two regions. Let R be the region containing the digon, with a small neighbourhood of S removed. Since the boundaries of the faces of \mathfrak{X}' are consistently oriented, the same is true for the portion of \mathfrak{X}' contained inside R , so this portion can be viewed as a (smaller) triple diagram. Suppose that U bounds a minimal interval within S (viewed as a portion of the boundary of R). Then by the induction assumption, U can be moved to be boundary-parallel to S . Since S and U are co-oriented, we get the picture on the left-hand side of (7.6.4) (with U running horizontally at the bottom). Applying (7.6.4), we obtain a monogon, a contradiction.

If the subinterval of S cut out by U is not minimal, then there is a strand T that cuts across S twice, creating a minimal interval within S and forming a digon inside R . We may assume that this digon is anti-parallel (or else replace U by T and repeat). By the induction assumption, we can apply swivel moves inside R to make T boundary-parallel to S . We then apply (7.6.1) to remove the digon, as shown in Figure 7.36. Repeating this

operation if necessary, we obtain a triple diagram in which U bounds a minimal interval within S ; we then argue as above to arrive at a contradiction.

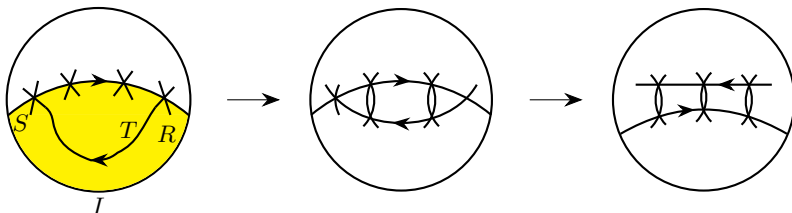


Figure 7.36. Removing double intersections with S .

Thus, no triple diagram $\mathfrak{X}' \sim \mathfrak{X}$ contains badgons. By Lemma 7.6.5, we conclude that any such \mathfrak{X}' does not contain closed strands either. This completes the induction step for statement (i).

We now proceed to proving statement (ii). In addition to the induction assumption for (ii), we may assume that neither \mathfrak{X} nor any triple diagram move-equivalent to \mathfrak{X} contains a badgon or a closed strand.

Let S be the strand connecting the endpoints of the minimal interval I . *Step 1: Removing double intersections with S , see Figure 7.36.* Let R be the region between the strand S and the interval I , with a small neighborhood of S removed. Suppose there is a strand that intersects S more than once. Among such strands, take one that cuts out a minimal interval along the boundary of R . Let T denote the segment of this strand contained in R . The portion of \mathfrak{X} contained inside R has fewer triple crossings than \mathfrak{X} , so by the induction assumption, we can make T boundary-parallel to S by applying swivel moves inside R . Now T and S form a (necessarily anti-parallel) digon, which we then remove using (7.6.1). We repeat this procedure until there are no strands left that intersect S more than once. Since the number of triple points along S decreases each time, the process terminates.

Step 2: Combing out the triple crossings. At this stage, no strand crosses S more than once. Since I is minimal, no strand has both ends at I . Since \mathfrak{X} contains no closed strands, every (non-self-intersecting) strand appearing between S and I must start or end at a point in I and cross S . Suppose that S is not boundary-parallel. Then there exists a strand T with an endpoint at I that passes through a triple point before hitting S . Among all such T , choose the one with the leftmost endpoint along I , cf. Figures 7.37 and 7.38 on the left. Let R be the part of the region between I and S that lies to the right of any strand T' located to the left of T . (By our choice of T , all such strands T' run directly from I to S , with no crossings in between.) As we have eliminated all double intersections with S , the interval corresponding to T (looking to the left) is minimal inside R . We can therefore use the induction assumption inside R to make T boundary-parallel.

What we do next depends on the orientation of T relative to S . If T is anti-parallel to S , as in Figure 7.37, then we apply (7.6.2) to make T run directly to S . If T is parallel to S , as in Figure 7.38, then we apply (7.6.3).

We repeat this step until S is boundary-parallel. \square

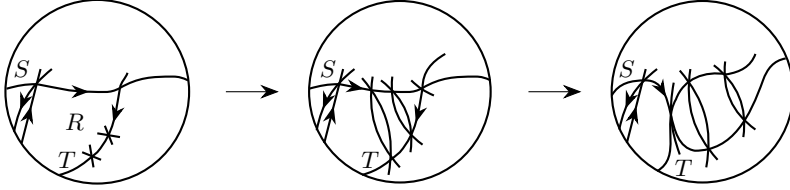


Figure 7.37. Combing out the triple crossings: the anti-parallel case.

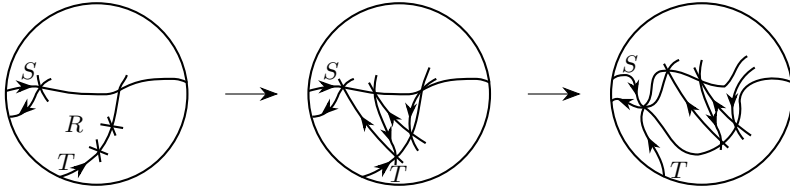


Figure 7.38. Combing out the triple crossings: the parallel case.

Lemma 7.6.12. *For a triple diagram \mathfrak{X} , the following are equivalent:*

- (a) *Any diagram \mathfrak{X}' move-equivalent to \mathfrak{X} does not contain a monogon.*
- (b) *\mathfrak{X} is move-equivalent to any standard triple diagram with the same strand permutation.*
- (c) *\mathfrak{X} is minimal.*

In particular, any standard triple diagram is minimal.

Proof. The implication (c) \Rightarrow (a) follows from Lemmas 7.6.3 and 7.6.6. To prove the implication (a) \Rightarrow (b), choose a sequence of minimal intervals and repeatedly apply Lemma 7.6.11. We have now established (c) \Rightarrow (b), so any minimal triple diagram is move-equivalent to any standard triple diagram with the same strand permutation. It follows by Lemma 7.6.3 that any standard triple diagram is minimal, hence so is any diagram move-equivalent to a standard one. Thus (b) \Rightarrow (c) is proved. \square

Proof of Theorem 7.6.2. By Lemma 7.6.12, any two minimal triple diagrams with strand permutation π are move-equivalent to any standard diagram with strand permutation π , and therefore to each other. \square

Lemma 7.6.13. *Let \mathfrak{X} and \mathfrak{X}' be triple diagrams related by a swivel move. If \mathfrak{X} contains a badgon, then so does \mathfrak{X}' .*

Proof. We label the strands and the triple points involved in this swivel move by a, b, c, d , and x, y , as shown in Figure 7.39.

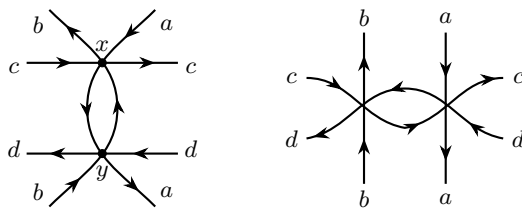


Figure 7.39. A swivel move relating \mathfrak{X} and \mathfrak{X}' .

If \mathfrak{X} contains a badgon that involves neither x nor y , then this badgon persists in \mathfrak{X}' .

Suppose \mathfrak{X} contains a monogon whose self-intersection point is (say) x . Thus, two of the strands $\{a, b, c\}$ coincide. If $a = c$ (resp., $b = c$), then the same monogon persists in \mathfrak{X}' because in Figure 7.39, strands a and c (resp., b and c) intersect in both \mathfrak{X} and \mathfrak{X}' .

If, on the other hand, $a = b$, then \mathfrak{X}' has a parallel digon, see Figure 7.40.

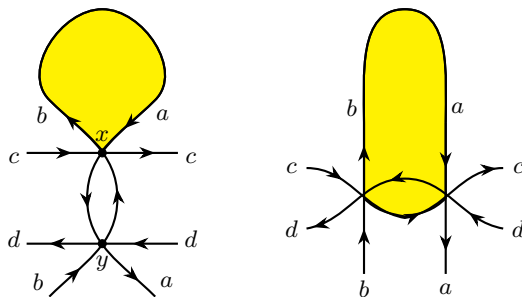


Figure 7.40. A monogon in \mathfrak{X} results in a parallel digon in \mathfrak{X}' .

From now on, we can assume that there is no monogon in \mathfrak{X} . Suppose \mathfrak{X} has a parallel digon whose two intersection points include x but not y . The sides of this parallel digon are either $\{a, b\}$ or $\{a, c\}$ or $\{b, c\}$. The last two cases are easy because such a parallel digon will persist in \mathfrak{X}' , since the strands a and c (resp., b and c) intersect in both \mathfrak{X} and \mathfrak{X}' .

Now suppose that our parallel digon has sides a and b , see Figure 7.41 on the left. (If the strands a and b go to the left and meet again there, then we get the same picture but with the roles of x and y interchanged.) Note that the end of strand a shown inside the digon must extend outside of it, but it cannot intersect a , as this would create a monogon. So strand a must intersect strand b again, see Figure 7.41 in the middle. Then, after the swivel move, we get a parallel digon as shown in Figure 7.41 on the right.

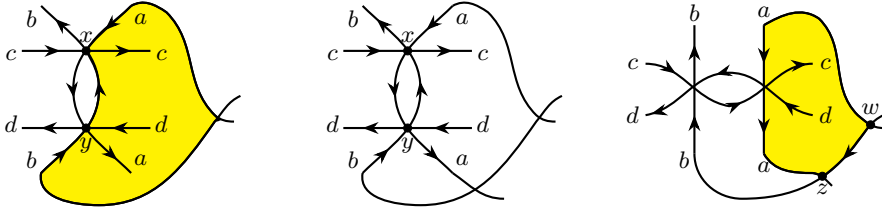


Figure 7.41. Persistence of parallel digons under swivel moves.

Finally, suppose there is a parallel digon in \mathfrak{X} whose two intersection points are x and y . We can assume it is oriented from x to y . The two sides of the parallel digon should come from the following list:

- (aa) the (portion of the) arc along a from x to y ;
- (bb) the arc along b from x to y ;
- (cd) an arc leaving x along c , and returning to y along d (so $c = d$);
- (cb) an arc leaving x along c , and returning to y along b (so $c = b$);
- (bd) an arc leaving x along b , and returning to y along d (so $b = d$).

In case (bb), we get a closed strand; it will persist in \mathfrak{X}' and yield a badgon by Lemma 7.6.5. In cases (cb) and (bd), we get a monogon, contradicting our assumption. The remaining case is when the parallel digon has sides (aa) and (cd); we then get a monogon in \mathfrak{X}' . (The picture is like Figure 7.40, with the roles of \mathfrak{X} and \mathfrak{X}' swapped and some strands relabeled.) \square

Theorem 7.6.14. *A triple diagram is minimal if and only if it has no badgons.*

Proof. The “only if” direction is Lemma 7.6.6. The “if” direction follows from Lemma 7.6.13 and Lemma 7.6.12 (implication (a) \Rightarrow (c)). \square

Lemma 7.6.15. *Assume that a triple diagram \mathfrak{X} is not minimal. Then there exists a diagram \mathfrak{X}' move-equivalent to \mathfrak{X} that contains a hollow monogon.*

Proof. We will argue by induction on the number of faces in \mathfrak{X} . If this number is 1 or 2, then the claim is vacuously true.

By Lemma 7.6.12, there exists $\mathfrak{X}' \sim \mathfrak{X}$ such that \mathfrak{X}' has a monogon. Let M be the segment of a strand in \mathfrak{X}' that forms a monogon; we may assume M does not intersect itself except at its endpoints (or else replace M by its subsegment). If the monogon encircled by M is hollow, we are done. Otherwise, consider the disk \mathbf{D}_\circ obtained by removing a small neighborhood of M from the interior of the monogon. Let \mathfrak{X}'_\circ denote the portion of \mathfrak{X}' contained in \mathbf{D}_\circ ; this is a triple diagram with fewer faces than \mathfrak{X}' (or equivalently \mathfrak{X}).

The rest of the argument proceeds by showing that either we can apply local moves to \mathfrak{X}'_\circ to create a hollow monogon inside \mathbf{D}_\circ or we can apply

moves to reduce the number of faces inside the monogon encircled by M (eventually producing a hollow monogon). If \mathfrak{X}'_{\circ} is not minimal, then the induction assumption applies, so we can transform \mathfrak{X}'_{\circ} (thus \mathfrak{X}' or \mathfrak{X}) into a move-equivalent triple diagram containing a hollow monogon. Therefore, we may assume that \mathfrak{X}'_{\circ} is minimal. Let M_{\circ} denote the interval obtained from the boundary of \mathbf{D}_{\circ} by removing a point located near the vertex of our monogon. Let $I \subset M_{\circ}$ be a minimal interval of the triple diagram \mathfrak{X}'_{\circ} . Since this triple diagram is minimal, we can, by Lemma 7.6.12 (or Lemma 7.6.11), apply local moves inside \mathbf{D}_{\circ} to transform \mathfrak{X}'_{\circ} into a triple diagram in which the strand T connecting the endpoints of I is boundary-parallel to I . Let us now look at the digon D formed by T and the portion of M that runs along I . If D is anti-parallel, then we can push T outside the monogon as in Figure 7.36, reducing the number of faces enclosed by M . If, on the other hand, D is parallel, then we can use (7.6.4) to create a hollow monogon. \square

7.7. From minimal triple diagrams to reduced plabic graphs

In this section, we use the machinery of triple diagrams and normal plabic graphs to prove Proposition 7.1.17, Theorem 7.1.23, and Corollary 7.1.25. In particular, we will be working with normal plabic graphs which are reduced and hence leafless, see Remark 7.5.9. It follows that all the machinery that we have developed for leafless reduced plabic graphs will apply here.

Recall from Definition 7.5.10 and Proposition 7.5.13 that the map $G \rightarrow \mathfrak{X}(G)$ gives a bijection between normal plabic graphs and triple diagrams with the same number of boundary vertices; moreover, this bijection preserves the associated (resp., trip or strand) permutation.

Theorem 7.7.1. *A normal plabic graph G is reduced if and only if the triple diagram $\mathfrak{X}(G)$ is minimal. Thus the map $G \mapsto \mathfrak{X}(G)$ restricts to a bijection between reduced normal plabic graphs and minimal triple diagrams.*

Proof. Suppose $\mathfrak{X}(G)$ is not minimal. By Lemma 7.6.15, there is a triple diagram $\mathfrak{X}' \sim \mathfrak{X}(G)$ such that \mathfrak{X}' has a hollow monogon. By Proposition 7.5.13, $\mathfrak{X}' = \mathfrak{X}(G')$ for some normal plabic graph G' . Moreover, Corollary 7.5.26 implies that $G \rightsquigarrow G'$. The hollow monogon in \mathfrak{X}' corresponds in the normal graph G' to one of the configurations shown in Figure 7.42: either a hollow digon (in which case by definition G' is not reduced) or a black leaf adjacent to a white trivalent vertex (in which case, as G' is normal, it is not reduced, by Remark 7.5.9). Either way, G' is not reduced, so G is not reduced either.

Going in the other direction, let G be a non-reduced normal plabic graph. Then either G has a (necessarily) black leaf or $G \sim G'$ where G' contains a hollow digon. By Lemma 7.5.25, the triple diagram $\mathfrak{X}(G)$ is move-equivalent to the (generalized) triple diagram $\mathfrak{X}(G')$. Since $\mathfrak{X}(G)$ is connected, so is $\mathfrak{X}(G')$. It follows by Lemma 7.5.24 that $\mathfrak{X}(G')$ is an honest triple diagram.

If G contains a black leaf, then $\mathfrak{X}(G)$ contains a monogon, cf. Figure 7.42, hence is not minimal. If G' contains a hollow digon with vertices of the same color, then $\mathfrak{X}(G')$ has a closed strand; hence $\mathfrak{X}(G')$ is not minimal (by Lemma 7.6.6) and neither is $\mathfrak{X}(G)$. If the vertices of the digon have different colors, cf. Figure 7.42, then $\mathfrak{X}(G')$ contains a monogon, hence is not minimal. \square

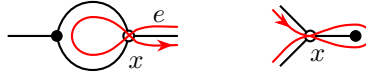


Figure 7.42. A hollow monogon in a triple diagram yields a forbidden configuration in the corresponding normal plabic graph.

Proof of Proposition 7.1.17. Let G be a reduced leafless plabic graph such that $\pi_G(i) = i$. We need to show that the connected component of G containing the boundary vertex i is a lollipop at i .

Suppose otherwise, that G has no lollipop at i . Without loss of generality we can assume that G has no lollipops at any other boundary vertex, since they don't affect which moves we can apply. By Definition 7.5.22, G is move-equivalent to a normal plabic graph G' . The trip permutations of G and G' coincide with each other (by Exercise 7.1.15) and with the strand permutation of the triple diagram $\mathfrak{X}(G')$ (by Proposition 7.5.13). Since G is reduced, so is G' ; hence $\mathfrak{X}(G')$ is minimal by Theorem 7.7.1.

Let d be the degree of the black vertex adjacent to the boundary vertex i in G' . It is impossible that $d = 1$, since moves (M1), (M2), (M3) never create degree 1 vertices. If $d = 2$ (see Figure 7.43 on the left), then $\pi_G(i) = i$ implies that $\mathfrak{X}(G')$ has a monogon, so it cannot be minimal, cf. Lemma 7.6.6. If $d \geq 3$, then we get a parallel digon (see Figure 7.43 on the right), again contradicting the minimality of $\mathfrak{X}(G')$. \square



Figure 7.43. The vicinity of i in G' .

Proof of Theorem 7.1.23. Let G and G' be reduced (leafless) plabic graphs. If $G \sim G'$, then $\tilde{\pi}_G = \tilde{\pi}_{G'}$ by Exercise 7.1.22. We need to show the converse.

Let G and G' be reduced (leafless) plabic graphs such that $\tilde{\pi}_G = \tilde{\pi}_{G'}$. If this decorated permutation has a fixed point at some vertex i , then by Proposition 7.1.17, applying local moves if needed, both G and G' have a lollipop of the same color in position i . Delete this lollipop in both

graphs; the resulting graphs are still reduced, and their decorated trip permutations coincide. So without loss of generality, we may assume that $\tilde{\pi}_G = \tilde{\pi}_{G'}$ has no fixed points and accordingly G and G' have no lollipops. Applying local moves as needed, we can furthermore assume, in light of Definition 7.5.22, that both G and G' are normal. Since they are reduced, Theorem 7.7.1 implies that the triple diagrams $\mathfrak{X}(G)$ and $\mathfrak{X}(G')$ are minimal. By Proposition 7.5.13, we moreover have $\pi_{\mathfrak{X}(G)} = \pi_G = \pi_{G'} = \pi_{\mathfrak{X}(G')}$. Invoking Theorem 7.6.2, we conclude that $\mathfrak{X}(G)$ and $\mathfrak{X}(G')$ are move-equivalent. By Theorem 7.5.21 and Lemma 7.5.20, the same is true for G and G' . \square

Proof of Corollary 7.1.25. Local moves do not change the number of faces. It follows by Theorem 7.1.23 that all reduced plabic graphs with a given decorated trip permutation have the same number of faces.

Changing the color of a lollipop transforms a reduced plabic graph into another reduced graph with the same number of faces and the same trip permutation (but with different decoration). Therefore all reduced plabic graphs G with $\pi(G) = \pi$ have the same number of faces.

It remains to show that if G is not reduced and has no internal leaves other than lollipops, then there exists a plabic graph G' with $\pi(G') = \pi$ and with fewer faces than G . Since G is not reduced, G can be transformed by local moves that do not create internal leaves into a plabic graph G'' containing a hollow digon. We claim that there exists a plabic graph G''' (not move-equivalent to G'') that has the same trip permutation as G'' , but fewer faces compared to G'' . The graph G''' is constructed as follows. If the vertices of the hollow digon in G'' are of the same color, then remove one of the sides of the digon (keeping its vertices) to get G''' . If, on the other hand, the vertices of the digon have different colors, then remove both sides of the digon; if one of the vertices was bivalent, then remove it as well. It is straightforward to check that in each case, the trip permutation does not change, whereas the number of faces decreases by 1 or 2. \square

Remark 7.7.2. As we have seen, A. Postnikov's theory of plabic graphs [22] is closely related to D. Thurston's theory of triple diagrams [25]. In particular, reduced plabic graphs are essentially minimal triple diagrams in disguise. If one starts with a non-reduced (leafless) plabic graph, one can apply the moves together with the reduction move (R1) in order to transform the graph into a reduced one. Similarly, one can apply reduction moves to a non-minimal triple diagram in order to eventually make it minimal. Here, however, the two theories diverge: reduction moves for triple diagrams preserve the strand permutation, but reduction moves for plabic graphs do not preserve the trip permutation. In spite of that, reduction for plabic graphs fits into the theory of the totally nonnegative Grassmannian, as it is compatible with its cell decomposition, cf. [22, Section 12]. We will discuss this in a subsequent chapter.

7.8. The bad features criterion

In this section, we provide a criterion for deciding whether a (leafless) plabic graph is reduced or not.

Lemma 7.8.1. *A reduced leafless plabic graph has no roundtrips.*

Proof. We may assume that our plabic graph G does not contain white lollipops. (Removing lollipops does not affect whether a graph is reduced or whether it has a roundtrip.) Since G is leafless, by Definition 7.5.22 it is move-equivalent to a normal plabic graph G' . Since G' is reduced, $\mathfrak{X}(G')$ is minimal (see Theorem 7.7.1). Hence $\mathfrak{X}(G')$ has no closed strands (see Lemma 7.6.6), so G' has no roundtrips. Since roundtrips persist under local moves, G has no roundtrips either. \square

Definition 7.8.2. If a trip passes through an edge e of a plabic graph twice (in the opposite directions), we call this an *essential self-intersection*.

If for two edges e_1 and e_2 , there are two distinct trips each of which passes first through e_1 and then through e_2 , we call this a *bad double crossing*.

We use the term *bad features* to collectively refer to

- roundtrips (see Definition 7.1.8),
- essential self-intersections, and
- bad double crossings.

These notions are illustrated in Figure 7.44.

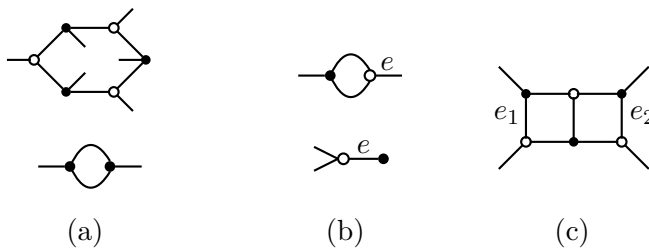


Figure 7.44. Plabic graph fragments representing “bad features:” (a) a roundtrip; (b) essential self-intersection; (c) bad double crossing. The fragment at the bottom of column (b) may not appear in a leafless plabic graph, but may occur in a normal plabic graph.

Lemma 7.8.3. *A normal plabic graph G has a bad feature if and only if the associated triple diagram $\mathfrak{X}(G)$ has a badgon.*

Proof. Let G be a normal plabic graph. The strands in the triple diagram $\mathfrak{X} = \mathfrak{X}(G)$ closely follow the trips in G . Therefore \mathfrak{X} has a closed strand if and only if G has a roundtrip.

If G has an essential self-intersection (resp., a bad double crossing), then \mathfrak{X} has a monogon (resp., a parallel digon). To see that, take each edge e involved in a bad feature and consider the white end v of e . The strands corresponding to the trips involved in the bad feature will intersect at v ; thus v will be a vertex of the corresponding badgon. Cf. Figures 7.42 and 7.45.

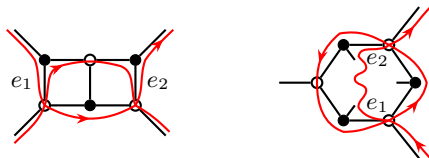


Figure 7.45. A bad double crossing in G yields a parallel digon in $\mathfrak{X}(G)$.

Conversely, suppose that \mathfrak{X} has a monogon with self-intersection corresponding to the white vertex v of G . There are three strand segments of \mathfrak{X} that pass through v , each running along two distinct edges incident to v ; because we have a self-intersection, two of these strands segments are part of the same strand s . Since v is trivalent, the pigeonhole principle implies that two of the four edges that s runs along must coincide. This yields an essential self-intersection in G . A similar argument shows that if \mathfrak{X} has a parallel digon, then G has a bad double crossing. \square

Corollary 7.8.4. *Let G be a normal plabic graph. Let $\mathfrak{X} = \mathfrak{X}(G)$ be the corresponding triple diagram. Then the following are equivalent:*

- G is reduced;
- \mathfrak{X} is minimal;
- G has no bad features;
- \mathfrak{X} has no badgons.

Proof. By Theorem 7.7.1, G is reduced if and only if \mathfrak{X} is minimal. By virtue of Theorem 7.6.14, \mathfrak{X} is minimal if and only if \mathfrak{X} has no badgons. By Lemma 7.8.3, \mathfrak{X} has no badgons if and only if G has no bad features. \square

The following result is a version of [22, Theorem 13.2].

Theorem 7.8.5. *A normal plabic graph is reduced if and only if it does not contain any bad features. A leafless plabic graph is reduced if and only if it does not contain any bad features.*

Proof. The first statement is a consequence of Corollary 7.8.4. The second statement follows from the first, using Definition 7.5.22, plus the fact that the moves relating a leafless plabic graph to a normal plabic graph neither add nor remove bad features. \square

For example, any plabic graph containing one of the fragments shown in Figure 7.44 is necessarily not reduced.

Remark 7.8.6. Recall from Remark 2.3.4 that an expression (possibly non-reduced) of an element of a symmetric group as a product of simple reflections can be represented by a wiring diagram. As plabic graphs can be viewed as generalizations of wiring diagrams (see Example 7.3.4), reduced plabic graphs may be viewed as a generalization of reduced expressions. In this context, the criterion of Theorem 7.8.5 corresponds to the condition that each pair of lines in the wiring diagram intersect at most once.

7.9. Affine permutations

By Theorem 7.1.23, move-equivalence classes of reduced plabic graphs are labeled by decorated permutations. An alternative labeling utilizes $((a, b)$ -bounded) *affine permutations*, introduced and studied in this section.

Definition 7.9.1. For a decorated permutation $\tilde{\pi}$ on b letters, we say that $i \in \{1, \dots, b\}$ is an *anti-excedance* of $\tilde{\pi}$ if either $\tilde{\pi}^{-1}(i) > i$ or $\tilde{\pi}(i) = \bar{i}$.

We will usually let a denote the number of anti-excedances.

Example 7.9.2. The decorated permutation $\tilde{\pi} = (5, \underline{2}, \bar{3}, 6, 4, 1)$ on $b = 6$ letters (cf. Figure 7.55) has $a = 3$ anti-excedances, namely, 3, 4, and 1.

Definition 7.9.3. Let $\tilde{\pi}$ be a decorated permutation on b letters with a anti-excedances. The *affinization* of $\tilde{\pi}$ is the map $\tilde{\pi}_{\text{aff}} : \mathbb{Z} \rightarrow \mathbb{Z}$ constructed as follows. For $i \in \{1, \dots, b\}$, we set

$$\tilde{\pi}_{\text{aff}}(i) = \begin{cases} \tilde{\pi}(i) & \text{if } \tilde{\pi}(i) > i, \\ i & \text{if } \tilde{\pi}(i) = \underline{i}, \\ \tilde{\pi}(i) + b & \text{if } \tilde{\pi}(i) < i, \\ i + b & \text{if } \tilde{\pi}(i) = \bar{i}. \end{cases}$$

We then extend $\tilde{\pi}_{\text{aff}}$ to \mathbb{Z} so that it satisfies

$$(7.9.1) \quad \tilde{\pi}_{\text{aff}}(i + b) = \tilde{\pi}_{\text{aff}}(i) + b \quad (i \in \mathbb{Z}).$$

We note that

$$(7.9.2) \quad i \leq \tilde{\pi}_{\text{aff}}(i) \leq i + b \quad (i \in \mathbb{Z}),$$

$$(7.9.3) \quad \sum_{i=1}^b (\tilde{\pi}_{\text{aff}}(i) - i) = b \cdot \#\{i \in \{1, \dots, b\} \mid \tilde{\pi}(i) < i \text{ or } \tilde{\pi}(i) = \bar{i}\} = ab.$$

Example 7.9.4. Continuing with $\tilde{\pi} = (5, \underline{2}, \bar{3}, 6, 4, 1)$ from Example 7.9.2, we get $\tilde{\pi}_{\text{aff}}(1) = 5$, $\tilde{\pi}_{\text{aff}}(2) = 2$, $\tilde{\pi}_{\text{aff}}(3) = 9$, $\tilde{\pi}_{\text{aff}}(4) = 6$, $\tilde{\pi}_{\text{aff}}(5) = 10$, $\tilde{\pi}_{\text{aff}}(6) = 7$, or more succinctly,

$$\tilde{\pi}_{\text{aff}} = (\dots, 5, 2, 9, 6, 10, 7, \dots) = (\dots \boxed{5 \ 2 \ 9 \ 6 \ 10 \ 7} \ 11 \ 8 \ 15 \ 12 \ 16 \ 13 \ \dots).$$

(The boxed terms are the values at $1, \dots, b$. They determine the rest of the sequence by virtue of (7.9.1).) In accordance with (7.9.3), we have

$$(5 + 2 + 9 + 6 + 10 + 7) - (1 + \dots + 6) = 39 - 21 = 18 = 3 \cdot 6 = ab.$$

With the above construction in mind, we introduce the following notion.

Definition 7.9.5. Let a and b be positive integers. An (a, b) -bounded affine permutation is a bijection $f : \mathbb{Z} \rightarrow \mathbb{Z}$ satisfying the following conditions:

- $f(i + b) = f(i) + b$ for all $i \in \mathbb{Z}$;
- $i \leq f(i) \leq i + b$ for all $i \in \mathbb{Z}$;
- $\sum_{i=1}^b (f(i) - i) = ab$.

Lemma 7.9.6. [16] The correspondence $\tilde{\pi} \mapsto \tilde{\pi}_{\text{aff}}$ (see Definition 7.9.3) restricts to a bijection between decorated permutations on b letters with a anti-excedances and the (a, b) -bounded affine permutations.

Lemma 7.9.6 is illustrated in Figure 7.46 (the first two columns).

$\tilde{\pi}$	$\tilde{\pi}_{\text{aff}}$	$\ell(\tilde{\pi}_{\text{aff}})$
$\overline{1} \underline{2} \underline{3}$	$\dots \boxed{4 \ 2 \ 3} \ 7 \ 5 \ 6 \ \dots$	2
$\underline{1} \overline{2} \underline{3}$	$\dots \boxed{1 \ 5 \ 3} \ 4 \ 8 \ 6 \ \dots$	2
$\underline{1} \underline{2} \overline{3}$	$\dots \boxed{1 \ 2 \ 6} \ 4 \ 5 \ 9 \ \dots$	2
$2 \ 1 \underline{3}$	$\dots \boxed{2 \ 4 \ 3} \ 5 \ 7 \ 6 \ \dots$	1
$\underline{1} \ 3 \ 2$	$\dots \boxed{1 \ 3 \ 5} \ 4 \ 6 \ 8 \ \dots$	1
$3 \underline{2} \ 1$	$\dots \boxed{3 \ 2 \ 4} \ 6 \ 5 \ 7 \ \dots$	1
$2 \ 3 \ 1$	$\dots \boxed{2 \ 3 \ 4} \ 5 \ 6 \ 7 \ \dots$	0

Figure 7.46. Decorated permutations $\tilde{\pi}$ on $b=3$ letters with $a=1$ anti-excedance; the corresponding (a, b) -bounded affine permutations $\tilde{\pi}_{\text{aff}}$; and the lengths $\ell(\tilde{\pi}_{\text{aff}})$ of these affine permutations, cf. Definition 7.9.8.

Proof. If $\tilde{\pi}$ is a decorated permutation on b letters with a anti-excedances, then (7.9.1)–(7.9.3) show that $\tilde{\pi}_{\text{aff}}$ is an (a, b) -bounded affine permutation.

Conversely, given an (a, b) -bounded affine permutation $f : \mathbb{Z} \rightarrow \mathbb{Z}$, we can define the decorated permutation $\tilde{\pi}$ on b letters by

$$\tilde{\pi}(i) = \begin{cases} \underline{i} & \text{if } f(i) = i; \\ \overline{i} & \text{if } f(i) = i + b; \\ f(i) & \text{if } f(i) \leq b \text{ and } f(i) \neq i; \\ f(i) - b & \text{if } f(i) > b \text{ and } f(i) \neq i + b. \end{cases}$$

We claim that $\tilde{\pi}$ has a anti-excedances. Using the inequality $i \leq f(i) \leq i + b$, we conclude that the anti-excedances of $\tilde{\pi}$ are in bijection with the values

$i \in \{1, \dots, b\}$ such that $f(i) > b$. The claim follows from the observation that $ab = \sum_1^b (f(i) - i) = b \cdot \#\{i \in \{1, \dots, b\} \mid f(i) > b\}$. \square

Recall from Exercise 7.1.19 that the number of decorated permutations on b letters is equal to $b! \sum_{k=0}^b \frac{1}{k!}$. We next refine this formula by taking into account the number of anti-excedances.

Let $D_{a,b}$ denote the number of decorated permutations on b letters with a anti-excedances (or the number of (a, b) -bounded affine permutations, cf. Lemma 7.9.6). The following result is reproduced here without a proof.

Proposition 7.9.7 ([22, Proposition 23.1]). *We have*

$$\sum_{0 \leq a \leq b} D_{a,b} x^a \frac{y^b}{b!} = e^{xy} \frac{x-1}{x - e^{y(x-1)}}.$$

Definition 7.9.8. An *inversion* of $\tilde{\pi}_{\text{aff}}$ is a pair of integers (i, j) such that $i < j$ and $\tilde{\pi}_{\text{aff}}(i) > \tilde{\pi}_{\text{aff}}(j)$. Two inversions (i, j) and (i', j') are *equivalent* if $i' - i = j' - j \in b\mathbb{Z}$. The *length* $\ell(\tilde{\pi}_{\text{aff}})$ of $\tilde{\pi}_{\text{aff}}$ is the number of equivalence classes of inversions. (We note that $\ell(\tilde{\pi}_{\text{aff}})$ equals the number $\text{align}(\tilde{\pi})$ of *alignments* of $\tilde{\pi}$, as defined in [22].) This number is finite since for any inversion (i, j) , we have $i < j < i + b$. Indeed, if $j \geq i + b$, then $\tilde{\pi}_{\text{aff}}(j) \geq j \geq i + b \geq \tilde{\pi}_{\text{aff}}(i)$. See Figure 7.46.

We will now state, without proof, a refinement of Proposition 7.9.7 that enumerates decorated permutations on b letters with respect to both the number of anti-excedances and the number of inversions. To this end, we set

$$D_{a,b}(q) = \sum_{\tilde{\pi}} q^{a(b-a) - \text{align}(\tilde{\pi})} = \sum_{\tilde{\pi}_{\text{aff}}} q^{a(b-a) - \ell(\tilde{\pi}_{\text{aff}})},$$

where the first sum is over all decorated permutations on b letters with a anti-excedances, and the second sum is over all (a, b) -bounded affine permutations. The significance of this polynomial is that the coefficient of q^r in $D_{a,b}(q)$ is the number of r -dimensional positroid cells in the totally nonnegative Grassmannian $\text{Gr}_{a,b}^{\geq 0}$, see [26].

Theorem 7.9.9 ([26, Theorem 4.1]). *We have*

$$D_{a,b}(q) = q^{-a^2} \sum_{i=0}^{a-1} (-1)^i \binom{b}{i} (q^{ai} [a-i] [a-i+1]^{b-i} - q^{(a+1)i} [a-i-1] [a-i]^{b-i}),$$

where we use the “ q -analogue” notation $[j] = 1 + q + q^2 + \dots + q^{j-1}$.

We next introduce an important special class of bounded affine permutations.

Definition 7.9.10. Let $\tilde{\pi}_{\text{aff}}$ be an (a, b) -bounded affine permutation, an affinization of a decorated permutation $\tilde{\pi}$, cf. Lemma 7.9.6. We refer to a position $i \in \mathbb{Z}$ such that $\tilde{\pi}_{\text{aff}}(i) \equiv i \pmod{b}$ (in other words, $\tilde{\pi}_{\text{aff}}(i) \in \{i, i+b\}$; and if $1 \leq i \leq b$ then $\tilde{\pi}(i) \in \{\underline{i}, \bar{i}\}$) as a *fixed point* of $\tilde{\pi}_{\text{aff}}$. If every $i \in \mathbb{Z}$ is a fixed point of $\tilde{\pi}_{\text{aff}}$, then we say that $\tilde{\pi}_{\text{aff}}$ is *equivalent to the identity modulo b* (or that $\tilde{\pi}$ is a *decoration of the identity*).

Lemma 7.9.11. *Let $\tilde{\pi}_{\text{aff}}$ be an (a, b) -bounded affine permutation that is equivalent to the identity modulo b . Then $\ell(\tilde{\pi}_{\text{aff}}) = a(b - a)$.*

Proof. Let $I = \{i \in \{1, \dots, b\} \mid \tilde{\pi}_{\text{aff}}(i) = i + b\}$ and $\underline{I} = \{i \in \{1, \dots, b\} \mid \tilde{\pi}_{\text{aff}}(i) = i\}$. Then $|I| = a$ and $|\underline{I}| = b - a$. The equivalence classes of inversions of $\tilde{\pi}_{\text{aff}}$ are described by the following list of representatives:

$$\{(i, j) \in I \times \underline{I} \mid 1 \leq i < j \leq b\} \cup \{(i, j + b) \mid (i, j) \in I \times \underline{I}, 1 \leq j < i \leq b\}.$$

The cardinality $\ell(\tilde{\pi}_{\text{aff}})$ of this set is equal to $|I \times \underline{I}| = a(b - a)$. \square

Lemma 7.9.12. *If $\tilde{\pi}_{\text{aff}}$ is not equivalent to the identity modulo b , then there exist $i, j \in \mathbb{Z}$ such that*

$$(7.9.4) \quad 1 \leq i < j \leq b,$$

$$(7.9.5) \quad \tilde{\pi}_{\text{aff}}(i) < \tilde{\pi}_{\text{aff}}(j),$$

$$(7.9.6) \quad \text{every position } h \text{ such that } i < h < j \text{ is a fixed point of } \tilde{\pi}_{\text{aff}}, \text{ and}$$

$$(7.9.7) \quad \text{neither } i \text{ nor } j \text{ are fixed points of } \tilde{\pi}_{\text{aff}}.$$

Proof. Suppose such a pair (i, j) does not exist. Let $i_1 < \dots < i_m$ be the elements of $\{1, \dots, b\}$ that are not fixed points of $\tilde{\pi}_{\text{aff}}$. Then

$$i_1 < \dots < i_m < \tilde{\pi}_{\text{aff}}(i_m) \leq \dots \leq \tilde{\pi}_{\text{aff}}(i_1).$$

We conclude that none of the values $\tilde{\pi}_{\text{aff}}(i_j)$ is of the form i_ℓ and consequently is of the form $i_\ell + b$. In particular, $\tilde{\pi}_{\text{aff}}(i_j) = i_m + b$ for some $j \neq m$. This implies $\tilde{\pi}_{\text{aff}}(i_j) > i_j + b$, a contradiction. \square

We next describe an algorithm for factoring affine permutations that will be used in Section 7.10.

Definition 7.9.13. Let $\tilde{\pi}_{\text{aff}}$ be an (a, b) -bounded affine permutation.

- If $\tilde{\pi}_{\text{aff}}$ is not equivalent to the identity modulo b , then use Lemma 7.9.12 to find positions $i, j \in \mathbb{Z}$ satisfying (7.9.4)–(7.9.7).
- Swap the values of $\tilde{\pi}_{\text{aff}}$ in positions i and j (and more generally, in positions $i + mb$ and $j + mb$, for all $m \in \mathbb{Z}$).
- Repeat this procedure until we obtain an affine permutation that is equivalent to the identity modulo b .

The ordered list of transpositions (ij) produced by the above algorithm is called the *bridge factorization* of $\tilde{\pi}_{\text{aff}}$.

An example of a bridge factorization is shown in Figure 7.47.

1	2	3	4	5	6	(i, j)	number of inversions
4	6	5	7	8	9		1
						(34)	
4	6	7	5	8	9		2
						(23)	
4	7	6	5	8	9		3
						(12)	
7	4	6	5	8	9		4
						(56)	
7	4	6	5	9	8		5
						(45)	
7	4	6	9	5	8		6
						(34)	
7	4	9	6	5	8		7
						(46)	
7	4	9	8	5	6		8
						(24)	
7	8	9	4	5	6		9

Figure 7.47. Applying the algorithm described in Definition 7.9.13 to the (a, b) -bounded affine permutation $\tilde{\pi}_{\text{aff}} = (4, 6, 5, 7, 8, 9)$, with $b = 6$ and $a = 3$. The resulting bridge factorization is the sequence $(34), (23), (12), (56), (45), (34), (46), (24)$. The entries corresponding to fixed points are boxed.

Remark 7.9.14. In view of (7.9.3), the affine permutation at hand remains (a, b) -bounded after each step of the algorithm in Definition 7.9.13. Moreover, the algorithm in Definition 7.9.13 terminates because each swap increases the length of the affine permutation by 1; this number is bounded by Definition 7.9.8.

Proposition 7.9.15. *Among all (a, b) -bounded affine permutations $\tilde{\pi}_{\text{aff}}$, the ones that have the maximal possible length $\ell(\tilde{\pi}_{\text{aff}}) = a(b - a)$ are precisely the ones that are equivalent to the identity modulo b .*

Proof. This follows from Lemma 7.9.11 and Remark 7.9.14. □

7.10. Bridge decompositions

Bridge decompositions [2, Section 3.2] provide a useful recursive construction of reduced plabic graphs with a given decorated trip permutation.

Definition 7.10.1. A *bridge* is a graph fragment shown in Figure 7.48 on the left. Let $\tilde{\pi}$ be a decorated permutation on b letters that has a anti-excedances, and let $\tilde{\pi}_{\text{aff}}$ be the corresponding affine permutation. To build a plabic graph associated to $\tilde{\pi}_{\text{aff}}$, we begin by introducing a white (resp., black) lollipop in each position i with $\tilde{\pi}(i) = \bar{i}$ (resp., $\tilde{\pi}(i) = \underline{i}$). If $\tilde{\pi}$ is a decoration of the identity, we are done. Otherwise, we use Definition 7.9.13 to produce a *bridge factorization*, then attach successive bridges in the corresponding positions, as in Figure 7.48. The resulting graph is called a *bridge decomposition* of $\tilde{\pi}_{\text{aff}}$, or sometimes a BCFW bridge decomposition, due to its relation with the Britto-Cachazo-Feng-Witten recursion in quantum field theory, see [2].

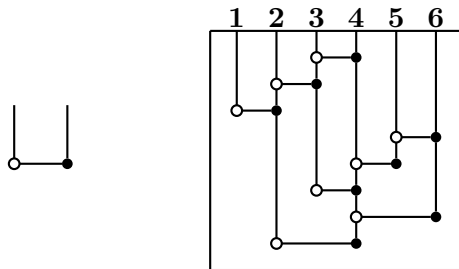


Figure 7.48. *Left:* a single bridge. *Right:* the bridge decomposition associated to the factorization constructed in Figure 7.47. The resulting plabic graph has trip permutation $\tilde{\pi} = (4, 6, 5, 1, 2, 3)$. Moreover, we have $\tilde{\pi} = (24)(46)(34)(45)(56)(12)(23)(34)$, the product of the transpositions (i, j) generated by the algorithm (reading right to left).

Proposition 7.10.2. A bridge decomposition of an (a, b) -bounded affine permutation $\tilde{\pi}_{\text{aff}}$ uses $a(b - a) - \ell(\tilde{\pi}_{\text{aff}})$ bridges.

Proof. See Lemma 7.9.11 and Definitions 7.9.13 and 7.10.1. □

Theorem 7.10.3. Let $\tilde{\pi}$ be a decorated permutation on b letters that has a anti-excedances. Let $\tilde{\pi}_{\text{aff}}$ be the associated (a, b) -bounded affine permutation. Then any bridge decomposition of $\tilde{\pi}_{\text{aff}}$ is a reduced plabic graph with the decorated trip permutation $\tilde{\pi}$.

Proof. We use induction on the number of bridges $\beta = a(b - a) - \ell(\tilde{\pi}_{\text{aff}})$. If $\beta = 0$, then $\tilde{\pi}$ is a decoration of the identity (see Proposition 7.9.15), so the bridge decomposition consists entirely of lollipops, and we are done.

Now suppose that $\tilde{\pi}$ is not a decoration of the identity. Proceeding as in Definition 7.9.13, we construct a bridge factorization $\sigma_1, \sigma_2, \dots, \sigma_\beta$,

where $\sigma_1 = (ij)$ satisfies (7.9.4)–(7.9.7). Let G be the plabic graph obtained by attaching bridges according to $\sigma_1, \dots, \sigma_\beta$ (from top to bottom). By the induction assumption, attaching bridges according to $\sigma_2, \dots, \sigma_\beta$ as in Definition 7.10.1 produces a reduced plabic graph G' with the trip permutation $\tilde{\pi}' = \sigma_\beta \cdots \sigma_2$. This graph has $\beta - 1$ bridges and is obtained by removing the topmost horizontal edge e from G and applying local moves (M2) to remove the endpoints of e .

Conversely, G is obtained from G' by attaching a bridge in position (i, j) at the top of G' . (To illustrate, in Figure 7.48 we have $(i, j) = (3, 4)$.) When we add this bridge to G' , the trips starting at i and j get their “tails” swapped: the trip T_i (resp., T_j) in G that begins at i (resp., at j) traverses e and continues along the trip that used to begin at j (resp., at i) in G' ; all other trips remain the same. Hence the trip permutation of G is $\tilde{\pi}'\sigma_1 = \tilde{\pi}$.

It remains to show that G is reduced. One option is to use the “bad features” criterion of Theorem 7.8.5. However, it will be more convenient for us to utilize the triple diagram version of the criterion, cf. Corollary 7.8.4.

We use Definition 7.5.22 to construct a normal graph $N(G)$ and the associated triple diagram $\mathfrak{X}(G) = \mathfrak{X}(N(G))$. The graph G is reduced if and only if $N(G)$ is reduced, which is equivalent to the triple diagram $\mathfrak{X} = \mathfrak{X}(G)$ being minimal, or to \mathfrak{X} having no badgons, see Corollary 7.8.4. Thus, our goal is to show \mathfrak{X} has no badgons.

By the induction assumption, the triple diagram $\mathfrak{X}' = \mathfrak{X}(G')$ has no badgons. It follows that any potential badgon in \mathfrak{X} must involve the white endpoint w of edge e ; otherwise this feature would have already been present in \mathfrak{X}' . In particular, this means that w is trivalent.

A monogon in \mathfrak{X} would have to have its vertex at w . Three of the six half-strands at w run straight to or from the boundary, so we need to use two of the remaining three; moreover, those two half-strands have to be oppositely oriented. There are two such cases to consider. In one case, i would be a fixed point of $\tilde{\pi}$, contradicting our choice of (i, j) . In the other case, i would be a fixed point of $\tilde{\pi}' = \tilde{\pi}(G')$, which can also be ruled out since in that case, i would not participate in any bridge in G' , making it impossible to produce the bottom vertex of the vertical edge pointing downwards from w .

Finally, suppose that \mathfrak{X} contains a parallel digon. One of the vertices of the digon has to be w ; let w' denote the other vertex. Since the two sides of the digon are oriented in the same way at w , it follows that these sides lie on the strands S_i and S_j that start near the vertices i and j , respectively.

By our choice of bridge (i, j) , every h with $i < h < j$ is a fixed point of $\tilde{\pi}$, but i and j are not fixed points. It follows that S_i (resp. S_j) does not terminate at i (resp. j), and neither terminates between the boundary vertices i and j . We explained in the monogon case that S_j cannot terminate at i ; one can similarly argue that S_i cannot terminate at j . Also, neither S_i

nor S_j intersects itself. Moreover the “tails” of S_i and S_j that start at the second vertex w' of the digon do not intersect each other (since otherwise a parallel digon would have been present in \mathfrak{X}'). It follows that either $\tilde{\pi}(i) < i$ and $\tilde{\pi}(j) > j$, or $\tilde{\pi}(i) > \tilde{\pi}(j) > j$, or $\tilde{\pi}(j) < \tilde{\pi}(i) < i$. In each case, we get $\tilde{\pi}_{\text{aff}}(i) > \tilde{\pi}_{\text{aff}}(j)$, which contradicts the way we chose i and j . \square

Corollary 7.10.4. *Let $\tilde{\pi}$ be a decorated permutation on b letters. Then there exists a reduced plabic graph whose decorated trip permutation is $\tilde{\pi}$.*

Proof. Use either Theorem 7.10.3 or the construction in Definition 7.6.8 (together with Proposition 7.5.13 and Theorem 7.7.1). \square

Corollary 7.10.5. *Let G be a reduced plabic graph with the decorated trip permutation $\tilde{\pi}$. If $\tilde{\pi}$ has b letters and a anti-excedances, then the number of faces in G is $a(b-a) - \ell(\tilde{\pi}_{\text{aff}}) + 1$.*

Proof. The number of faces is invariant under local moves. Therefore, by Theorem 7.1.23, it suffices to establish this formula for a particular reduced plabic graph with decorated trip permutation $\tilde{\pi}$. By Theorem 7.10.3, we can use a bridge decomposition of $\tilde{\pi}_{\text{aff}}$. Since each bridge adds one face to the graph, the claim follows by Proposition 7.10.2. \square

Let $\tilde{\pi}_{a,b}$ denote the decorated permutation on b letters defined by

$$(7.10.1) \quad \tilde{\pi}_{a,b} = \begin{cases} (a+1, a+2, \dots, b, 1, 2, \dots, a) & \text{if } 1 \leq a \leq b-1 \\ (1, 2, \dots, a) & \text{if } a = 0 \\ (\bar{1}, \bar{2}, \dots, \bar{a}) & \text{if } a = b \end{cases}$$

Exercise 7.10.6. Let $\tilde{\pi}$ be a decorated permutation on b letters that has a anti-excedances. Show that if $\ell(\tilde{\pi}_{\text{aff}}) = 0$, then $\tilde{\pi} = \tilde{\pi}_{a,b}$.

Corollary 7.10.7. *Let G be a reduced plabic graph whose decorated trip permutation $\tilde{\pi}_G$ has b letters and a anti-excedances. Then G has at most $a(b-a) + 1$ faces. Moreover it has $a(b-a) + 1$ faces if and only if $\tilde{\pi}_G = \tilde{\pi}_{a,b}$.*

Proof. This is immediate from Corollary 7.10.5 and Exercise 7.10.6. \square

Remark 7.10.8. The *permutohedron* \mathcal{P}_n [24, Exercise 4.64a] is a polytope whose $n!$ vertices are labeled by permutations in the symmetric group \mathcal{S}_n . Shortest paths in the 1-skeleton of \mathcal{P}_n encode reduced expressions in \mathcal{S}_n , and its 2-dimensional faces correspond to their local (braid) transformations, cf. Exercise 7.3.9. Similarly, paths in the 1-skeleton of the *bridge polytope* [27] encode bridge decompositions of the decorated permutation $\tilde{\pi}_{a,b}$; its 2-dimensional faces correspond to local moves in plabic graphs.

7.11. Edge labels of reduced plabic graphs

Definition 7.11.1. Let G be a leafless plabic graph. Let us label the edges of G by subsets of integers that indicate which one-way trips traverse a given edge; more precisely, for each boundary vertex i , we include i in the label of every edge contained in the trip that starts at i . By Remark 7.1.13, each edge will be labeled by at most two integers. See Figure 7.49.

We say that G has the *resonance property* if after labeling the edges of G as in Definition 7.11.1, the following condition is satisfied at each internal vertex v that is not a lollipop:

- there exist numbers $i_1 < \dots < i_m$ such that the edges incident to v are labeled by the two-element sets $\{i_1, i_2\}, \{i_2, i_3\}, \dots, \{i_{m-1}, i_m\}, \{i_1, i_m\}$, appearing in clockwise order.

In particular, each edge of G that is not incident to a lollipop is labeled by a two-element subset. See Figure 7.49.

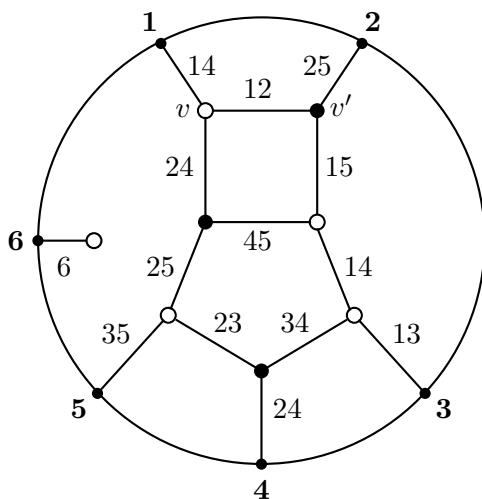


Figure 7.49. A reduced plabic graph from Figures 7.1(b) and 7.6. Its edge labeling exhibits the resonance property, see Definition 7.11.1. For example, the edge labels around the vertex v (resp., v'), listed in clockwise order, are $\{1, 2\}, \{2, 4\}, \{1, 4\}$ (resp., $\{1, 2\}, \{2, 5\}, \{1, 5\}$).

Remark 7.11.2. At a bivalent vertex v , the resonance condition is satisfied if and only if the two trips passing through v are distinct and none of them is a roundtrip.

Remark 7.11.3. If a plabic graph G is trivalent (apart from lollipops), then the resonance property is equivalent to the following requirement at each interior vertex v (other than a lollipop):

- the three edges incident to v have labels $\{a, b\}$, $\{a, c\}$, and $\{b, c\}$, for some $a < b < c$, and moreover this (lexicographic) ordering of labels corresponds to the counterclockwise direction around v .

For example, in Figure 7.49, the edge labels around the vertex v (resp., v') are, in lexicographic order, $\{1, 2\}, \{1, 4\}, \{2, 4\}$ (resp., $\{1, 2\}, \{1, 5\}, \{2, 5\}$). The three edges carrying these labels appear in the counterclockwise order around v (resp., v').

Exercise 7.11.4. Verify that none of the plabic graphs shown in Figure 7.44 (draw a disk around each of the fragments) satisfy the resonance property.

Theorem 7.11.5 ([17, Theorem 10.5]). *Let G be a leafless plabic graph. Then G is reduced if and only if it has the resonance property.*

Theorem 7.11.5 is proved below in this section, following a few remarks and auxiliary lemmas.

Remark 7.11.6. We find the resonance criterion of Theorem 7.11.5 easier to check than the “bad features” criterion of Theorem 7.8.5.

Remark 7.11.7. Certain reduced plabic graphs were realized as tropical curves in [17], where it was shown that the resonance property corresponds to the *balancing condition* for tropical curves.

Lemma 7.11.8. *The resonance property is preserved under the local moves (M1)–(M3).*

Proof. The square move (M1) only changes the labels of the sides of the square, see Figure 7.50. Moreover, the labels around each vertex match the labels around the opposite vertex after the square move, with the same cyclic order. Hence this move preserves the resonance property.

The case of the local move (M2) is easy, cf. Remark 7.11.2.

For the case of the local move (M3) around a degree 4 black vertex, see Figure 7.51. (The case of white vertices and of higher degree vertices of both colors is similar.) \square

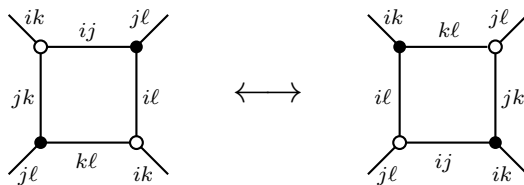


Figure 7.50. Transformation of edge labels under a square move (M1).

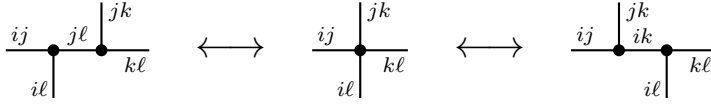


Figure 7.51. Transformation of edge labels under a local move (M3) at a 4-valent black vertex. (Alternatively, make all the vertices white.)

Lemma 7.11.9. *Any plabic graph obtained via the bridge decomposition construction (see Definition 7.10.1) has the resonance property.*

Proof. We will show that, more concretely, the edge labels around trivalent vertices in such a plabic graph G follow one of the patterns described in Figure 7.52. We will establish this result by induction on β , the number of bridges, following the strategy used in the proof of Theorem 7.10.3.

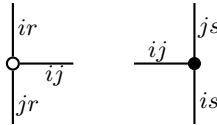


Figure 7.52. Edge labels near trivalent vertices in a bridge decomposition. At a white vertex, shown on the left, either $r < i < j$ or $i < j < r$. At a black vertex, shown on the right, either $s < i < j$ or $i < j < s$.

Let G be a bridge decomposition of $\tilde{\pi}_{\text{aff}}$, associated to the sequence of transpositions $\sigma_1, \dots, \sigma_\beta$. Thus $\tilde{\pi} = \tilde{\pi}_G = \sigma_\beta \cdots \sigma_1$. Here $\sigma_1 = (ij)$, where i and j satisfy (7.9.4)–(7.9.7). Let G' be the bridge decomposition associated to $\sigma_2, \dots, \sigma_\beta$, so that G is obtained from G' by adding a single bridge in position (i, j) at the top of G' .

Suppose the result is true for G' . We need to verify it for G . Let $r = \tilde{\pi}^{-1}(i)$ and $s = \tilde{\pi}^{-1}(j)$. Adding the bridge in position (i, j) at the top of G' adds at most two trivalent vertices: it adds a white (respectively, black) trivalent vertex provided that $r \neq j$ (respectively, $s \neq i$). The cases when one of the vertices on the bridge is bivalent are easy to verify, so we are going to assume that $r \neq j$ and $s \neq i$. In this case, the local configuration around positions i and j in G' and G is as shown in Figure 7.53.

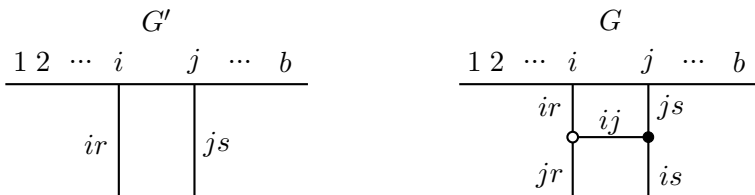


Figure 7.53. The local configuration around positions i and j in G' and G .

Recall that $i < j$ and moreover any h such that $i < h < j$ is a fixed point of $\tilde{\pi}$. For the reasons indicated in the proof of Theorem 7.10.3, adding the bridge (i, j) at the top of G' has the effect of replacing the label i (resp., j) by j (resp., i) in every edge label outside of the bridge.

If G' has an edge with the label ij , then G has a bad double crossing involving the trips originating at i and j . This however is impossible since G is reduced, by Theorem 7.10.3. Therefore G' has no edge with label ij . Furthermore, G' has no edge with a label h for $i < h < j$. Since all trivalent vertices of G' satisfy the resonance condition of Figure 7.52, the same remains true after switching the labels i and j . Thus, all trivalent vertices of G that were present in G' satisfy this resonance condition.

Finally, the two new trivalent vertices in G satisfy this condition because $i < j$ and we can exclude $i < r < j$ and $i < s < j$ because of (7.9.6). \square

Proof of Theorem 7.11.5. We first establish the “if” direction. Let G be a leafless plabic graph. Suppose that G has the resonance property. We want to show that G is reduced.

Assume the contrary. By definition, G can be transformed by local moves (that is, (M1), (M2), (M3)) into a plabic graph G' containing a hollow monogon or a hollow digon. Since G has the resonance property, so does G' , by Lemma 7.11.8. This yields a contradiction because the labels around a hollow monogon or digon do not satisfy the resonance property, see Figure 7.54.

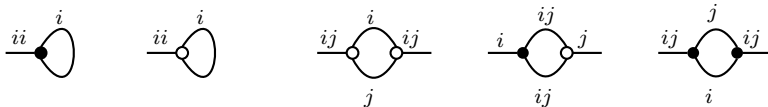


Figure 7.54. A plabic graph containing a hollow digon fails to satisfy the resonance property.

We next establish the “only if” direction. Suppose that G is reduced, with $\tilde{\pi}_G = \tilde{\pi}$. We know from Theorem 7.10.3 that there is a bridge decomposition G' —a reduced plabic graph—with trip permutation $\tilde{\pi}$. By Lemma 7.11.9, G' has the resonance property. By Theorem 7.1.23, $G \sim G'$. But now by Lemma 7.11.8, the resonance property is preserved under the local moves, so G has the resonance property as well. \square

7.12. Face labels of reduced plabic graphs

In this section, we use the notion of a trip introduced in Definition 7.1.8 to label each face of a reduced (leafless) plabic graph by a collection of positive integers. These face labels generalize the labeling of diagonals in a polygon by Plücker coordinates (cf. Section 1.2) as well as the labeling of faces in (double or ordinary) wiring diagrams by chamber minors (cf. Sections 1.3–1.4). In a subsequent chapter, we will relate the face labels of reduced plabic graphs to Plücker coordinates that form an extended cluster for the standard cluster structure on a Grassmannian or, more generally, on a Schubert or positroid subvariety within it.

Remark 7.12.1. Let G be a reduced (leafless) plabic graph. Let T_i be the one-way trip in G that begins at a boundary vertex i and ends at a boundary vertex j .

If $i \neq j$, then we claim that there are two kinds of faces in G : those on the left side of the trip T_i and those on the right side of it. This claim follows from the fact (see Theorem 7.8.5) that G does not contain essential self-intersections.

If $i = j$, then by Proposition 7.1.17, the boundary vertex i is incident to a lollipop. If this lollipop is white (resp., black), then we declare that all faces of G lie on the left (resp., right) side of the trip T_i .

Definition 7.12.2. Let G be a reduced (leafless) plabic graph with boundary vertices $1, \dots, b$. We define two natural face labelings of G , cf. Figure 7.55:

- in the *source labeling* $\mathcal{F}_{\text{source}}(G)$, each face f of G is labeled by the set

$$I_{\text{source}}(f) = \{i \mid f \text{ lies to the left of the trip starting at vertex } i\};$$

- in the *target labeling* $\mathcal{F}_{\text{target}}(G)$, each face f of G is labeled by the set

$$I_{\text{target}}(f) = \{i \mid f \text{ is to the left of the trip ending at vertex } i\}.$$

Remark 7.12.3. The edge labeling and the face labeling of a reduced plabic graph G are related as follows: if two faces f and f' of G are separated by a single edge whose edge label is $\{i, j\}$, then the face label of f' is obtained from that of f by either removing i and adding j , or removing j and adding i .

Theorem 7.12.4. Let G be a reduced (leafless) plabic graph with b boundary vertices. Let a denote the number of anti-excedances in the trip permutation π_G . Let us label the faces of G using either the source or the target labeling. Then every face of G will be labeled by an a -element subset of $\{1, \dots, b\}$.

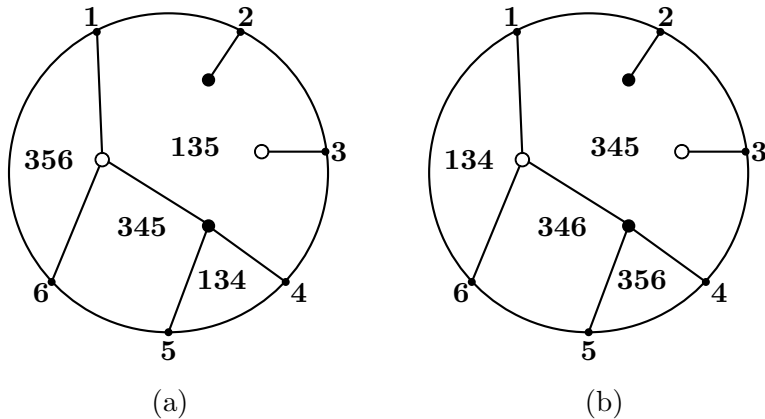


Figure 7.55. (a) The source labeling $\mathcal{F}_{\text{source}}(G)$ of a reduced plabic graph G . (b) The target labeling $\mathcal{F}_{\text{target}}(G)$. Here $\tilde{\pi}_G = (5, \underline{2}, \bar{3}, 6, 4, 1)$. Every face is labeled by a subset of cardinality 3, in agreement with Theorem 7.12.4, cf. Example 7.9.2.

Proof. By Theorem 7.11.5, every reduced (leafless) plabic graph G has the resonance property, which in particular means that every edge label of G consists of two distinct numbers. It then follows from Remark 7.12.3 that every face label of G has the same cardinality. It remains to show that this cardinality is a , the number of anti-excedances of $\tilde{\pi} = \tilde{\pi}_G$.

Furthermore, it is sufficient to establish the latter claim for one particular reduced plabic graph with the trip permutation $\tilde{\pi}_G$, e.g., for a bridge decomposition of $\tilde{\pi}_{\text{aff}}$. Indeed, any two reduced plabic graphs with the same trip permutation are related by local moves, and any such move preserves all labels except at most one, see Exercise 7.12.5.

To prove the theorem for bridge decompositions, we use induction on the number of bridges β . In the base case $\beta = 0$, the bridge decomposition G consists of a white lollipops, $b - a$ black lollipops, and no bridges. Thus G has a single face, labeled by the a -element subset indicating the positions of the white lollipops.

Consider a bridge decomposition G built from a bridge decomposition G' by adding a bridge in position (i, j) at the top of G' , as in Figure 7.53. Both G and G' have trip permutations with a anti-excedances (cf. Remark 7.9.14), so by the induction assumption, the faces in G' have cardinality a . Since G inherits most of its faces from G' , and all face labels of G have the same cardinality, this cardinality is equal to a . \square

Exercise 7.12.5. Verify that applying a move (M2) or (M3) does not affect the face labels of a plabic graph, whereas applying the square move (M1) changes the face labels as shown in Figure 7.56.

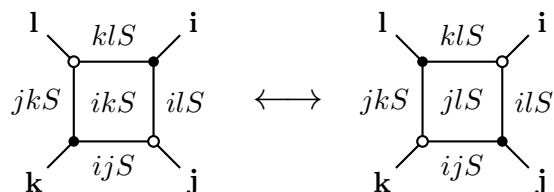


Figure 7.56. The effect of the square move (M1) on the face labeling. Here i, j, k, l are the (source or target) labels of the trips that traverse the outer edges towards the central square; S is an arbitrary set of labels disjoint from $\{i, j, k, l\}$; and abS is a shorthand for the set $\{a, b\} \cup S$.

The face labelings of plabic graphs can be used to recover the labelings of diagonals in a polygon by Plücker coordinates as well as the labelings of chambers in (ordinary or double) wiring diagrams by minors:

Exercise 7.12.6. Let T be a triangulation of a convex m -gon \mathbf{P}_m , and let $G(T)$ be the plabic graph defined in Example 7.3.1. Explain how to label the boundary vertices of $G(T)$ in such a way that the face labeling of $G(T)$ recovers the labeling of diagonals of \mathbf{P}_m by pairs of integers. Cf. Figure 7.57.

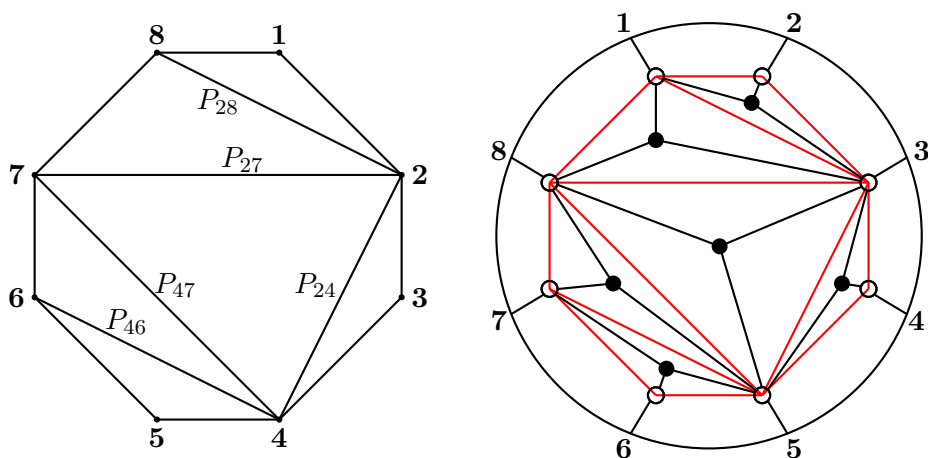


Figure 7.57. A triangulation T of an octagon and the corresponding plabic graph $G(T)$, cf. Figure 2.2.

Exercise 7.12.7. Let D be a wiring diagram with m wires. Let $G(D)$ be the plabic graph defined in Example 7.3.4, see also Figure 7.58. Label the boundary vertices of $G(D)$ by the numbers $1, \dots, 2m$ in the clockwise order, starting with a 1 at the lower left boundary vertex of $G(D)$. Label the faces of $G(D)$ using the source labeling $\mathcal{F}_{\text{source}}(G)$. Show that intersecting each face label with the set $\{1, 2, \dots, m\}$ recovers the labeling of D by chamber minors. See Figure 7.58.

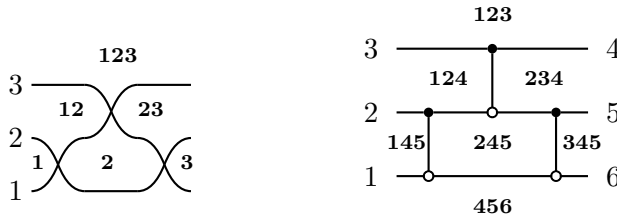


Figure 7.58. A wiring diagram D and the plabic graph $G(D)$ with the source labeling of its faces.

Exercise 7.12.8. Let D be a double wiring diagram with m pairs of wires. Let $G(D)$ be the plabic graph defined in Example 7.3.11. Label the boundary vertices of $G(D)$ by the numbers

$$1, 2, \dots, m-1, m, m', \dots, 2', 1'$$

in clockwise order, starting with the label 1 at the lower left boundary vertex of $G(D)$. Label the faces of $G = G(D)$ using the source labeling $\mathcal{F}_{\text{source}}(G)$, so that each face gets labeled by $I' \cup J$, where $I' \subset \{1', \dots, m'\}$ and $J \subset \{1, \dots, m\}$. Let I denote the set obtained from I' by replacing each i' by i . Show that mapping each face label $I' \cup J$ to the pair $([1, m] \setminus I, J)$ recovers the labeling of D by chamber minors. See Figure 7.59.

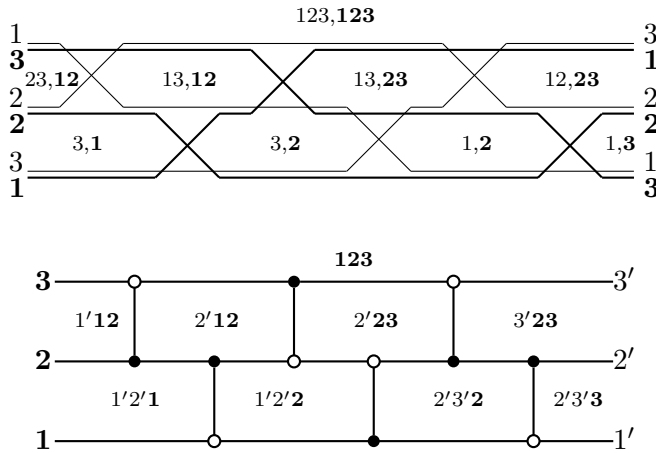


Figure 7.59. Double wiring diagram labeling from plabic graphs. The labeling of a double wiring diagram D is obtained from the source labeling of the associated plabic graph $G(D)$ using the recipe described in Exercise 7.12.8.

7.13. Grassmann necklaces and weakly separated collections

Fix two nonnegative integers b and $a \leq b$. We denote by $\binom{[b]}{a}$ the set of all a -element subsets of $\{1, \dots, b\}$.

In this section, we provide an intrinsic combinatorial characterization of the subsets of $\binom{[b]}{a}$ that arise as sets of face labels of reduced plabic graphs. The proofs are omitted.

Definition 7.13.1 ([19]). We say that two a -element subsets $I, J \in \binom{[b]}{a}$ are *weakly separated* if and only if, after drawing the numbers $1, 2, \dots, b$ clockwise around a circle, there exists a chord separating the sets $I \setminus J$ and $J \setminus I$ from each other. More specifically, I and J are weakly separated if there do not exist $i, j, i', j' \in \{1, \dots, b\}$ such that

- $i < j < i' < j'$ or $j < i < j' < i'$;
- $i, i' \in I \setminus J$ and $j, j' \in J \setminus I$.

Theorem 7.13.2 ([5, 20]). Let I and J be target face labels of two faces in a reduced plabic graph. Alternatively, let I and J be source face labels of two faces in a reduced plabic graph. Then I and J are weakly separated.

Definition 7.13.3. A collection $\mathcal{C} \subset \binom{[b]}{a}$ of a -element subsets of $[b]$ is *weakly separated* if any $I, J \in \mathcal{C}$ are weakly separated. Thus, Theorem 7.13.2 asserts that the collection of target (or source) face labels of a reduced plabic graph is weakly separated. A weakly separated collection \mathcal{C} is called *maximal* if it is not contained in any other weakly separated collection. See Figure 7.60.

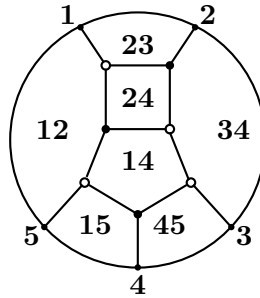


Figure 7.60. The target face labeling of the reduced plabic graph G from Figure 7.1(a). The set of labels $\{12, 23, 34, 45, 15, 24, 14\}$ is a maximal weakly separated collection in $\binom{[5]}{2}$. Here $\tilde{\pi}_G = \tilde{\pi}_{2,5} = (3, 4, 5, 1, 2)$.

Theorem 7.13.4 ([5, 20]). For $\mathcal{C} \subset \binom{[b]}{a}$, the following are equivalent:

- \mathcal{C} is a maximal weakly separated collection;
- \mathcal{C} is the set of target face labels of a reduced plabic graph G with $\tilde{\pi}_G = \tilde{\pi}_{a,b}$ (see (7.10.1)).

In that case, the cardinality of \mathcal{C} is equal to $|\mathcal{C}| = a(b - a) + 1$.

Remark 7.13.5. A general formula for the number of maximal weakly separated collections in $\binom{[b]}{a}$ is unknown. For $a = 2$, the maximal weakly separated collections in $\binom{[b]}{2}$ are in bijection with triangulations of a convex b -gon, so they are counted by the Catalan numbers C_{b-2} , where $C_n = \frac{1}{n+1} \binom{2n}{n}$. For $a = 3$ and $b = 6, \dots, 12$, the number of maximal weakly separated collections in $\binom{[b]}{3}$ is equal to 34, 259, 2136, 18600, 168565, 1574298, 15051702. See [6] for more data.

Theorem 7.13.4 can be generalized to arbitrary reduced plabic graphs. To state this result, we will need the following notion.

Definition 7.13.6 ([22, Definition 16.1]). A *Grassmann necklace* of type (a, b) is a sequence $\mathcal{I} = (I_1, \dots, I_b)$ of subsets $I_i \in \binom{[b]}{a}$ such that, for $i = 1, \dots, b$, we have $I_{i+1} \supset I_i \setminus \{i\}$. (Here the indices are taken modulo b , so that $I_1 \supset I_b \setminus \{b\}$.) Thus, if $i \notin I_i$, then $I_{i+1} = I_i$.

In other words, either $I_{i+1} = I_i$ or I_{i+1} is obtained from I_i by deleting i and adding another element. Note that if $I_{i+1} = I_i$, then either i belongs to all elements I_j of the necklace, or i belongs to none of them.

Example 7.13.7. The sequence $\mathcal{I} = (126, 236, 346, 456, 156, 126)$ is a Grassmann necklace of type $(3, 6)$.

Definition 7.13.8. For $\ell \in \{1, \dots, b\}$, we define the linear order $<_\ell$ on $\{1, \dots, b\}$ as follows:

$$\ell <_\ell \ell + 1 <_\ell \ell + 2 <_\ell \dots <_\ell b <_\ell 1 <_\ell \dots <_\ell \ell - 1.$$

For a decorated permutation $\tilde{\pi}$ on b letters, we say that $i \in \{1, \dots, b\}$ is an ℓ -anti-excedance of $\tilde{\pi}$ if either $\tilde{\pi}^{-1}(i) >_\ell i$ or if $\tilde{\pi}(i) = \bar{i}$. Thus, a 1-anti-excedance is the same as an (ordinary) anti-excedance, as in Definition 7.9.1.

It is not hard to see that the number of ℓ -anti-excedances does not depend on the choice of $\ell \in \{1, \dots, b\}$, so we simply refer to this quantity as the number of anti-excedances.

Lemma 7.13.9. *Decorated permutations on b letters with a anti-excedances are in bijection with Grassmann necklaces \mathcal{I} of type (a, b) .*

Proof. To go from \mathcal{I} to the corresponding decorated permutation $\tilde{\pi} = \tilde{\pi}(\mathcal{I})$, we set $\tilde{\pi}(i) = j$ whenever $I_{i+1} = (I_i \setminus \{i\}) \cup \{j\}$ for $i \neq j$. If $i \notin I_i = I_{i+1}$ then $\tilde{\pi}(i) = \bar{i}$, and if $i \in I_i = I_{i+1}$ then $\tilde{\pi}(i) = \bar{i}$.

Going in the other direction, let $\tilde{\pi}$ be a decorated permutation. For $\ell \in \{1, \dots, b\}$, we denote by I_ℓ the set of ℓ -anti-excedances of $\tilde{\pi}$. Then $\mathcal{I} = \mathcal{I}(\tilde{\pi}) = (I_1, \dots, I_b)$ is the corresponding Grassmann necklace. \square

Example 7.13.10. Let $\mathcal{I} = (126, 236, 346, 456, 156, 126)$, cf. Example 7.13.7. Then $\tilde{\pi}(\mathcal{I}) = (3, 4, 5, 1, 2, \bar{6})$.

Example 7.13.11. Let $\tilde{\pi}_G = \tilde{\pi}_{a,b}$, cf. (7.10.1). The corresponding Grassmann necklace (cf. Lemma 7.13.9) is given by

$$(7.13.1) \quad \mathcal{I}(\tilde{\pi}_{a,b}) = (\{1, 2, \dots, a\}, \{2, 3, \dots, a, a+1\}, \dots, \{b, 1, 2, \dots, a-1\}).$$

Definition 7.13.12. We extend the linear order $<_\ell$ on $\{1, \dots, b\}$ to a partial order on $\binom{[b]}{a}$, as follows. Let

$$\begin{aligned} I &= \{i_1, \dots, i_a\}, & i_1 <_\ell i_2 <_\ell \dots <_\ell i_a; \\ J &= \{j_1, \dots, j_a\}, & j_1 <_\ell j_2 <_\ell \dots <_\ell j_a. \end{aligned}$$

Then, by definition, $I \leq_\ell J$ if and only if $i_1 \leq_\ell j_1, \dots, i_a \leq_\ell j_a$.

Definition 7.13.13. For a Grassmann necklace $\mathcal{I} = (I_1, \dots, I_b)$ of type (a, b) , we define the associated *positroid* $\mathcal{M}_{\mathcal{I}}$ by

$$\mathcal{M}_{\mathcal{I}} = \{J \in \binom{[b]}{a} \mid I_\ell \leq_\ell J \text{ for all } \ell \in \{1, \dots, b\}\}.$$

As we will see in a subsequent chapter, positroids are the (realizable) *matroids* that arise from full rank $a \times b$ matrices with all Plücker coordinates nonnegative. Abstractly, one may also define a *positively oriented matroid* to be an oriented matroid on $\{1, 2, \dots, b\}$ whose chirotope takes nonnegative values on any ordered subset $\{i_1 < \dots < i_a\}$. By [1], these two notions are the same, in other words, every positively oriented matroid is realizable.

Example 7.13.14. Let $\mathcal{I} = \mathcal{I}(\tilde{\pi}_{a,b})$, see (7.13.1). Then $\mathcal{M}_{\mathcal{I}} = \binom{[b]}{a}$, i.e., the positroid associated with \mathcal{I} contains all a -element subsets of $\{1, \dots, b\}$.

Definition 7.13.15. Two reduced plabic graphs are called *strongly equivalent* if they have the same sets of face labels.

We note that two plabic graphs which are connected via moves (M2) and (M3) are strongly equivalent.

Recall that $\mathcal{F}_{\text{target}}(G)$ denotes the collection of target-labels of faces of a reduced plabic graph G .

Theorem 7.13.16 ([20, Theorem 1.5]). *Fix a decorated permutation $\tilde{\pi}$ on b letters with a anti-excedances. Let \mathcal{I} be the corresponding Grassmann necklace of type (a, b) , cf. Lemma 7.13.9. Let $\mathcal{M}_{\mathcal{I}}$ be the associated positroid, cf. Definition 7.13.13. Then the map $G \mapsto \mathcal{F}_{\text{target}}(G)$ gives a bijection between*

- the strong equivalence classes of reduced plabic graphs G with decorated trip permutation $\tilde{\pi}_G = \tilde{\pi}$ and
- the collections $\mathcal{C} \subset \binom{[b]}{a}$ that are maximal (with respect to inclusion) among the weakly separated collections satisfying $\mathcal{I} \subseteq \mathcal{C} \subseteq \mathcal{M}_{\mathcal{I}}$.

Remark 7.13.17. Let $\mathcal{I} = \mathcal{I}(\tilde{\pi}_{a,b})$. Then $\mathcal{I} = \mathcal{I}(\tilde{\pi}_{a,b})$ is given by (7.13.1). Each of the b cyclically consecutive subsets in (7.13.1) is weakly separated from every other a -element subset of $\{1, \dots, b\}$, so every maximal weakly separated collection $\mathcal{C} \subset \binom{[b]}{a}$ must contain \mathcal{I} . Furthermore, $\mathcal{M}_{\mathcal{I}} = \binom{[b]}{a}$ (see Example 7.13.14), so any such \mathcal{C} automatically satisfies the inclusions $\mathcal{I} \subseteq \mathcal{C} \subseteq \mathcal{M}_{\mathcal{I}}$. We thus recover Theorem 7.13.4 as a special case of Theorem 7.13.16.

Bibliography

- [1] ARDILA, F., RINCÓN, F., AND WILLIAMS, L. Positively oriented matroids are realizable. *J. Eur. Math. Soc. (JEMS)* 19, 3 (2017), 815–833.
- [2] ARKANI-HAMED, N., BOURJAILY, J., CACHAZO, F., GONCHAROV, A., POSTNIKOV, A., AND TRNKA, J. *Grassmannian geometry of scattering amplitudes*. Cambridge University Press, Cambridge, 2016.
- [3] BOCKLANDT, R. Calabi-Yau algebras and weighted quiver polyhedra. *Math. Z.* 273, 1-2 (2013), 311–329.
- [4] BROOMHEAD, N. Dimer models and Calabi-Yau algebras. *Mem. Amer. Math. Soc.* 215, 1011 (2012), viii+86.
- [5] DANILOV, V. I., KARZANOV, A. V., AND KOSHEVOY, G. A. On maximal weakly separated set-systems. *J. Algebraic Combin.* 32, 4 (2010), 497–531.
- [6] EARLY, N. From weakly separated collections to matroid subdivisions. *Comb. Theory* 2, 2 (2022), Paper No. 2, 35.
- [7] FOCK, V., AND GONCHAROV, A. Moduli spaces of local systems and higher Teichmüller theory. *Publ. Math. Inst. Hautes Études Sci.*, 103 (2006), 1–211.
- [8] FOMIN, S., IGUSA, K., AND LEE, K. Universal quivers. *Algebr. Comb.* 4, 4 (2021), 683–702.
- [9] FOMIN, S., PYLYAVSKYY, P., SHUSTIN, E., AND THURSTON, D. Morsifications and mutations. *J. Lond. Math. Soc. (2)* 105, 4 (2022), 2478–2554.
- [10] FOMIN, S., AND WILLIAMS, L. Introduction to Cluster Algebras. Chapter 7, version 2. arXiv:2106.02160v2.
- [11] GALASHIN, P. Plabic graphs and zonotopal tilings. *Proc. Lond. Math. Soc. (3)* 117, 4 (2018), 661–681.
- [12] HARER, J. L. The virtual cohomological dimension of the mapping class group of an orientable surface. *Invent. Math.* 84, 1 (1986), 157–176.
- [13] HATCHER, A. On triangulations of surfaces. *Topology Appl.* 40, 2 (1991), 189–194.
- [14] KAWAMURA, T. Links associated with generic immersions of graphs. *Algebr. Geom. Topol.* 4 (2004), 571–594.
- [15] KENYON, R. An introduction to the dimer model. In *School and Conference on Probability Theory*, ICTP Lect. Notes, XVII. Abdus Salam Int. Cent. Theoret. Phys., Trieste, 2004, pp. 267–304.

- [16] KNUTSON, A., LAM, T., AND SPEYER, D. E. Positroid varieties: juggling and geometry. *Compos. Math.* 149, 10 (2013), 1710–1752.
- [17] KODAMA, Y., AND WILLIAMS, L. KP solitons and total positivity for the Grassmannian. *Invent. Math.* 198, 3 (2014), 637–699.
- [18] KODAMA, Y., AND WILLIAMS, L. K. KP solitons, total positivity, and cluster algebras. *Proc. Natl. Acad. Sci. USA* 108, 22 (2011), 8984–8989.
- [19] LECLERC, B., AND ZELEVINSKY, A. Quasicommuting families of quantum Plücker coordinates. In *Kirillov’s seminar on representation theory*, vol. 181 of *Amer. Math. Soc. Transl. Ser. 2*. Amer. Math. Soc., Providence, RI, 1998, pp. 85–108.
- [20] OH, S., POSTNIKOV, A., AND SPEYER, D. E. Weak separation and plabic graphs. *Proc. Lond. Math. Soc. (3)* 110, 3 (2015), 721–754.
- [21] OH, S. H., AND SPEYER, D. E. Links in the complex of weakly separated collections. *J. Comb.* 8, 4 (2017), 581–592.
- [22] POSTNIKOV, A. Total positivity, Grassmannians, and networks, [arXiv:math/0609764](https://arxiv.org/abs/math/0609764).
- [23] POSTNIKOV, A. Positive Grassmannian and polyhedral subdivisions. In *Proceedings of the International Congress of Mathematicians—Rio de Janeiro 2018. Vol. IV. Invited lectures* (2018), World Sci. Publ., Hackensack, NJ, pp. 3181–3211.
- [24] STANLEY, R. P. *Enumerative combinatorics. Vol. 1*, second ed., vol. 49 of *Cambridge Studies in Advanced Mathematics*. Cambridge University Press, Cambridge, 2012.
- [25] THURSTON, D. P. From dominoes to hexagons. In *Proceedings of the 2014 Maui and 2015 Qinhuangdao conferences in honour of Vaughan F. R. Jones’ 60th birthday* (2017), vol. 46 of *Proc. Centre Math. Appl. Austral. Nat. Univ.*, Austral. Nat. Univ., Canberra, pp. 399–414. Preprint versions: [arXiv:math/0405482](https://arxiv.org/abs/math/0405482) (2004 and 2016).
- [26] WILLIAMS, L. K. Enumeration of totally positive Grassmann cells. *Adv. Math.* 190, 2 (2005), 319–342.
- [27] WILLIAMS, L. K. A positive Grassmannian analogue of the permutohedron. *Proc. Amer. Math. Soc.* 144, 6 (2016), 2419–2436.